Measurement of Ribozyme Cleavage Reaction Using Toehold Mediated Strand Displacement; Design, Validation and Possible Applications

Jay Kapadia

A Thesis in the Department of Engineering and Computer Engineering

Presented for the degree of Master's in Applied Science, Electrical and computer engineering,

Concordia University, Montreal, Quebec, Canada

April 2020

CONCORDIA UNIVERSITY
SCHOOL OF GRADUATE STUDIES

This is to certify that the thesis prepared

By: Jay Kapadia

Entitled: Measurement of Ribozyme Cleavage Reaction Using Toehold Mediated Strand
         Displacement; Design, Validation and Possible Applications

and submitted in partial fulfillment of the requirements for the degree of

Master of Applied Science (Electrical and Computer Engineering)

complies with the regulations of this University and meets the accepted standards with respect to
originality and quality.

Signed by the final examining committee:

_____ Chair
        Dr. S. Shih

_____ External Examiner
        Dr. A. Kachroo (BIOL)

_____ Internal Examiner
        Dr. S. Shih

_____ Co-Supervisor
        Dr. N. Kharma

_____ Co-Supervisor
        Dr. J. Perreault (INRS)

Approved by: _____
        Dr. Y.R. Shayan, Chair
        Department of Electrical and Computer Engineering

8th May 2020   _____
                     Dr. M. Debbabi, Interim Dean,
                 Faculty of Engineering and Computer Science

ABSTRACT

Measurement of Ribozyme Cleavage Reaction Using Toehold Mediated Strand

Displacement; Design, Validation and Possible Applications

Jay Kapadia

Non-coding RNAs or ncRNAs are RNA molecules that are not translated but play functional roles within cells. Some of these ncRNAs possess enzymatic properties. These molecules are termed as ribozymes. Ribozymes mainly catalyze nucleic acid strand scission reactions with or without the help of protein molecules. Ribozymes such as hammerhead ribozymes (HHRs) are known to mediate gene silencing and RNA processing. Single stranded RNA/DNA (ssRNA/DNA) inducible HHRs or tetracycline inducible aptazymes exist. Using these HHRs, different types of logic gates can be designed, activated by one or more inputs including ssDNA and ssRNA. Evaluating HHR kinetics of cleavage is essential to understand their mechanism, characterize HHR mutants and to properly estimate several parameters important to design RNA-based logic circuits.

Firstly, we developed a novel methodology to detect HHR kinetics using toehold mediated strand displacement reaction (TMSDR). A probe composed of a fluorophore and a quencher was designed to measure the kinetics of HHR cleavage reactions without labelling RNA molecules, regular sampling or the utilization of polyacrylamide gels. This probe consists of two DNA strands; one strand labelled with a fluorophore at its 5′ end, while the other strand labelled with a quencher at its 3′ end. These two DNA strands are complementary, but the fluorophore strand is longer than the quencher strand at its 3′. The unpaired extra nucleotides act as toehold, which is utilized by a

detached cleaved fragment, coming from a self-cleaving hammerhead ribozyme, as the starting point for the strand displacement reaction. This reaction will cause the separation of the fluorophore strand from the quencher strand, culminating in fluorescence detectable in a plate reader. This fluorescence is proportional to the amount of detached cleaved-off RNA strand displacing the DNA quencher strand. This method can be used to replace radio-hazardous unstable ^{32}P as a means of measurement of the kinetics of ribozyme cleavage reactions; it also eliminates the need for use of polyacrylamide gels for the same purpose. Critically, this method allows experimenters to distinguish between the amount of cleaved ribozyme and the amount of detached cleaved-off fragments, resulting from the cleavage.

Secondly, we developed doubler HHRs that cleave twice upon induction with a single input strand (ssDNA/ssRNA). Outputs can be heterogeneous (Hetero doubler) or identical (Homo doubler). Homo doublers were designed to work as amplifying components in RNA amplifiers. We showed two potential doubler HHRs from two different designs (First doubler and D1 doubler). In conclusion, we found that the concentration of detached cleaved-off fragments is relatively low and hence we developed homo-doublers to increase the concentration of cleaved-off fragments.

Acknowledgements

Table of Contents

List of Tables

List of Figures

Abbreviations

Abs: Absorbance

AMP: Adenosine monophosphate

ATP: Adenosine triphosphate

BHQ: Black hole quencher

BPB: Bromophenol blue

CTP: Cytosine triphosphate

CV: Converter

Cy5: Cyanine-5

DB: doubler

DNA: Deoxyribonucleic acid

dsDNA: double stranded DNA

EA: Evolutionary algorithm

EDTA: Ethylenediaminetetraacetic acid

Ex: Excitation

FRET: Florescence resonance energy transfer

GTP: Guanosine triphosphate

HEPES: 4-(2-hydroxyethyl)-1-piperazineethanesulfonic acid

HHR: Hammerhead ribozyme

MFE: Minimum free energy

μM: Micromole

mM: millimole

mRNA: messenger-RNA

ncRNA: non-coding RNA

nt: nucleotides

OBS: Oligonucleotide binding site

PCR: polymerase chain reaction

RNA: Ribonucleic acid

rNTP: ribonucleotide triphosphate

ssDNA: single-stranded DNA

ssRNA: single stranded RNA

TBMg: Tris-borate Mg

TMSDR: Toehold mediated strand displacement reaction

UTP: Uridine triphosphate

UV: Ultraviolet

XC: Xylene cyanole

Chapter 1 Introduction and Background

1.1 Nucleic acid

Nucleic acids are the principle informative molecules present in every cell. Deoxyribonucleic acid (DNA) is a prime molecule that transfer hereditary traits from one generation to another. DNA is a double helix polymer containing four bases, Adenine (A), Guanine (G), Cytosine (C) and Thymine (T). A and G are purine bases and C and T are pyrimidine bases and all these bases are linked by phosphorylated pentose sugar (ribose) as described in Figure 1 [1].
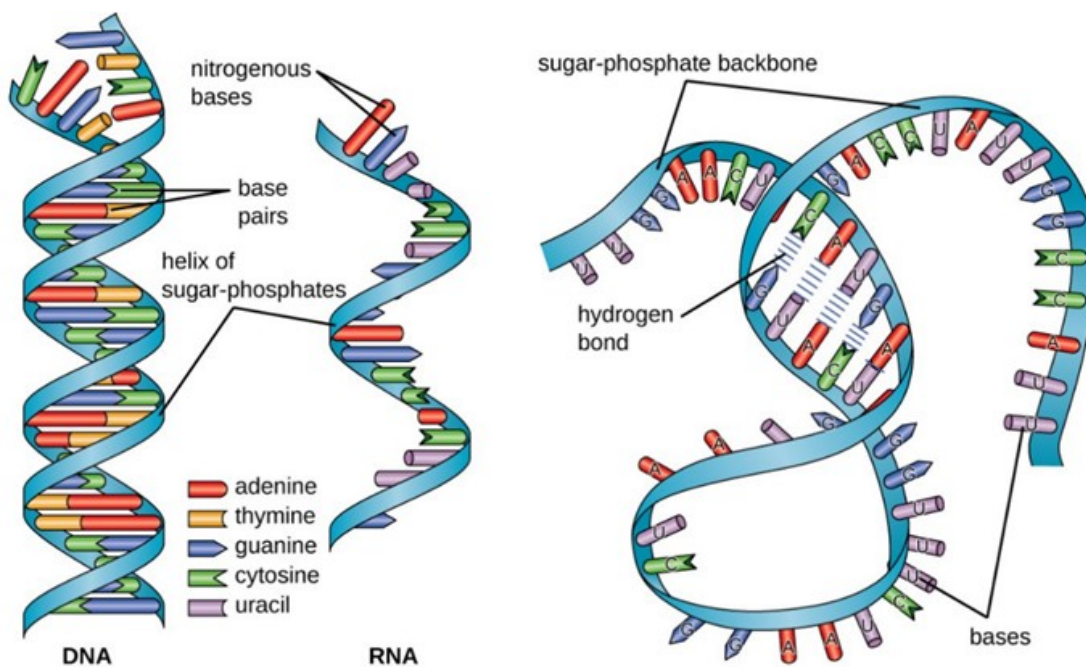
Figure 1. Nucleic acid structure

Illustration of DNA molecule (Far left) and RNA molecules (both single stranded molecules). Image adapted from [1, 2]

In DNA, the 2′ hydroxyl group is absent from the ribose sugar and hence, its termed as deoxyribose sugar. The A, T, G or C base is attached to the carbon 1′ of deoxyribose nucleosides. These nucleosides attached to a phosphate group on the 5′ oxygen are known as nucleotides [1].

1.2 Ribonucleic acid (RNA)

RNA is the abbreviation of Ribonucleic acid. RNA is similar in structure to DNA, but instead of a long perfectly double-stranded nucleic acid, it is a single stranded molecule with Uracil (U) replacing Thymine (T) [1, 3]. Another difference between DNA and RNA is the sugar, in case of DNA it is a deoxyribose sugar while in case of RNA it is a ribose sugar [1].

One of the key differences between DNA and RNA is that the latter is usually found in Nature as a single stranded molecule, which allows it to fold into various three-dimensional structures [1]. Another difference is the extra hydroxyl group on the C2 carbon, as opposed to hydrogen for DNA. This extra hydroxyl group gives RNA the capability to take part in various enzymatic reactions and it will make it prone to spontaneous degradation in alkaline solutions in contrast to DNA, which is stable in them [1, 4]. In RNA molecules, a G can base-pair with U, resulting in a G-U *wobble* base-pair. This pairing can be observed in all kinds of RNA structures present in all three domains of life. A G-U base pair is thermodynamically similar to both A-U and G-C base pairs, but it has unique chemical and ligand binding and other properties [1, 3, 4]. As described in Figure 1, RNA is, by default, a single stranded polynucleotide, which makes it much more flexible than usually double-stranded DNA molecules (such as those of chromosomes), allowing single-stranded (or ss) RNA to form various secondary and tertiary structures [1]. Examples of simple structures that an RNA molecule can form are hairpins, loops and bulges [1]. These structures are similar, but different from, the secondary structures of proteins, such as alpha-helices and beta-sheets. Similarly, when two or more simple RNA structural elements are put together, they can form more complex tertiary structures with diverse functions, such as cleavage and ligation, both playing roles in catalytic reactions [4]. Catalytic RNA molecules are called *ribozymes* and they play crucial roles in various cellular functions.

1.3 Ribozymes

Ribozymes are single stranded RNA molecules that can catalyze various reactions with or without the help of 'helper' proteins. The discovery of ribozymes can be traced back to the early eighties and from then, RNA chemical catalysis helped to explain certain biological processes like RNA splicing, RNA processing and replication and peptide bond formation during translation. Known natural ribozymes, except for the ribosome, catalyze phosphodiester ligation or cleavage reactions of RNA strands. The specific reaction catalyzed by a ribozyme is based on specific base pairing between substrate and ribozyme as well as other tertiary interactions [5, 6]. This selective interaction of ribozymes with other RNA molecules affords them considerable potential to inactivate specific transcripts of genes, resulting in gene silencing [7, 8].

Naturally occurring ribozymes contain a core region, which is comprised of conserved nucleotides that catalyze intramolecular reactions (except RNAse P) [7]. These ribozymes can act in *cis* and *trans* manner. *Trans* acting ribozymes act as true enzymes and they can interact with multiple substrate molecules. *Cis* acting ribozymes catalyze only one reaction [9]. These ribozymes can be divided into three categories: A) Self-splicing introns which can be further divided into groups I and II, B) RNAse P and last C) small catalytic RNAs ranging from 50-150 nucleotides. Our focus will be on the small catalytic RNA ribozymes of group I, because of their diversity and ease of manipulation in laboratory conditions. This group includes the hammerhead ribozyme (the workhorse of this study), the hairpin ribozyme, the hepatitis delta virus (HDV) ribozyme and the Varkud Satellite (VS) ribozyme [7-9].

1.4 Hammerhead ribozyme

Hammerhead ribozymes (HHRs) are small catalytic RNA motifs ranging from 50-150 nucleotides

that can act either as *cis-* or *trans*-acting agents, self-cleaving or cleaving target RNA molecules, respectively [10, 11]. Natural HHRs were identified in plant satellite RNA and viroids, where they process long RNA transcripts containing multimeric genomes to yield individual genomic RNAs [11]. The HHR is capable of catalyzing self-scission of phosphodiester backbone by the biochemical reaction termed as transesterification reaction [6]. HHR does not require any other molecule to catalyze the transesterification reaction but the literature suggests that divalent metal ions play an essential or at least positive role in a cleavage reaction [6, 12, 13]. The magnesium ion is the most prevalent divalent metal ion that facilitates the cleavage of HHR. [13] suggest that Mg^{2+} stabilizes the structure of HHR and will help to facilitate the strand scission reaction. HHRs have been studied extensively for past three decades because of their small size and robust activity *in vitro,* which makes them ideal model ribozymes for the study of the tertiary structure of RNA molecules, with significant implications for its activity [11].

As illustrated in Figure 2, HHR comprised of a 'core' of 15 conserved nucleotides (shown in red and black) and three helices (called stems) that merge to form the 'core'. The stems position and stabilize the core, which is essential for strand scission by internal phosphoester transfer reaction [10, 11]. Natural HHRs contain additional sequences which aide folding into an optimal tertiary structure where stem I and stem II interact; this increases the activity of the core by several orders of magnitude [14, 15]. These natural HHRs are known as *extended* hammerhead ribozymes while the minimal stem structure HHRs are known as *minimal* hammerhead ribozymes [16].

Figure 2. Consensus sequence of minimal hammerhead ribozyme.
Nucleotides in red are most conserved, nucleotides in black are conserved. N represents any nucleotide. I, II and III in bold represent stem numeration. Optional loop determines the type of hammerhead ribozyme (Type I, II or III). Figure taken from [11].

1.5 Inducible hammerhead ribozymes

Naturally occurring minimal hammerhead ribozymes have been used as models to produce synthetic ribozymes that can self-cleave to release a desired RNA strand or act as trans-acting enzymes to cleave a target RNA (e.g., mRNA) molecule [17, 18]. These synthetic ribozymes can be modeled to act like logic gates. A logic gate is a circuit (as in the case of a digital circuit) having one or more inputs and one output [17]. To create a YES gate using a hammerhead ribozyme, the ribozyme can be designed in such a way that when a DNA oligonucleotide binds the ribozyme (as 'input'), it will modulate the folding of the ribozyme, causing it to fold into an active conformation, facilitating the strand scission reaction illustrated in Figure 3. The strand scission reaction culminates in the release of small fragments termed as 'output'. The output of the ribozyme (acting

as a logic gate) can act as an input to the next ribozyme (perhaps, another logic gate) in a larger circuit. This allows for experimenters that create a wide array of molecular digital circuits that communicate with output strands to perform complex operations in a biological context [17, 19].
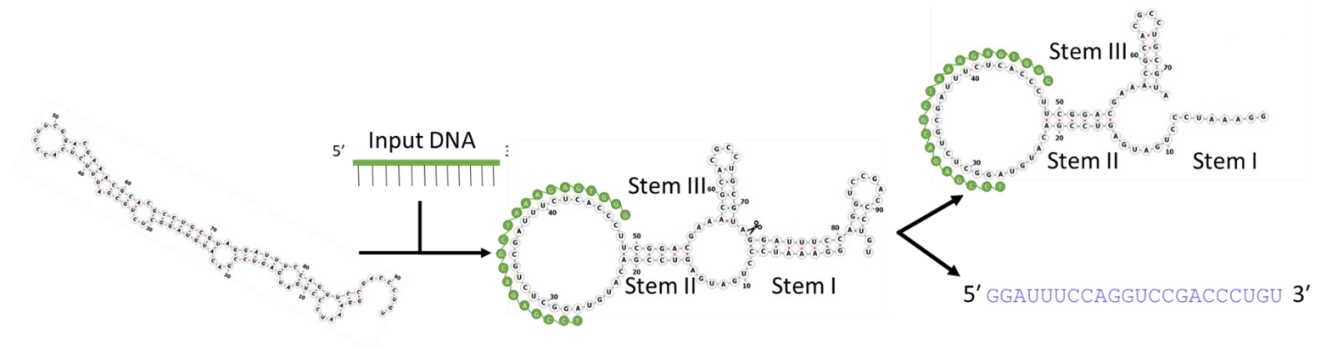
Figure 3. Inducible hammerhead ribozyme (YES logic gate)

Misfolded ribozyme induced by input DNA oligo (green) culminates in self-cleavage releasing a small RNA fragment and cleaved HHR bound with input.

1.6 Ribozyme kinetics

In the past decade, several methods have been developed and used to analyze and evaluate the structure, function, and activity of ribozymes *in vitro.* Established methods to analyze RNA molecules *in vitro* typically utilize the radioisotope ^{32}P, that can be incorporated during transcription or post transcriptionally using a kinase enzyme [11, 20]. This method involves cumbersome sampling for each kinetic data point and separation of cleavage products on denaturing polyacrylamide gels. [20, 21] To detect the cleavage, polyacrylamide gels are revealed by phosphorimaging [20, 21]. In addition to several disadvantages, like limited half-life or radiation hazard, the requirement of radioisotopes for this procedure limits it to laboratories with the appropriate facilities, which tend to be fewer and less common, as fluorescence tends to replace radioactivity as a preferred means of labeling. Other methods include post transcriptional fluorescence labelling, phsophoramidite chemistry of chemically synthesized RNA and engineered fluorescent aptamer designs (e.g., Spinach and Mango) [5, 20-22]. However, these methods are associated with direct RNA modification, which in turn impact the structure, function and thermodynamic stability of the measured ribozyme [21, 23, 24].

1.7 Review of approaches to measurement of hammerhead ribozyme kinetics using fluorescence

As described in the previous section, ribozymes, especially minimal hammerhead ribozymes are building blocks for designing logic circuits in bacterial, yeast and mammalian cells [5, 25]. One way to detect hammerhead ribozyme cleavage without radiolabelling is to attach a fluorescent aptamer and measure the change in fluorescence upon cleavage. The Spinach aptamer based complementation assay was used to measure the progress of a hammerhead ribozyme cleavage reaction *in vitro* without the use of radioactivity [5]. However, this approach leads to the modification of the ribozyme sequence, as one must incorporate an aptamer into one of the stems

of the hammerhead ribozyme [5]. This change affects the folding of the ribozyme, which might well modify the activity of the ribozyme.

A second approach, as described in [21], involves labelling RNA molecules during *in vitro* transcription. This approach takes advantage of the T7 φ2.5 promoter, resulting in RNA molecules that are labelled with cyanine AMP at their 5′ end [21]. [21] synthesized two novel cyanine-AMP conjugates, which can be incorporated by the T7 RNA polymerase during transcription, eliminating the need of a separate labelling step. This method eliminates the need for major sequence modifications of the RNA and allows for one step labelling. Cyanine dyes have excellent molar extinction coefficients and they resist photobleaching well [26]. However, one drawback of this technique is that the labeled RNA molecule must have an AG at its 5′ end [21]. Also, one needs to analyze the RNA products on a gel, which is cumbersome for large numbers of RNA samples and does not allow for automation.

FRET (fluorescence resonance energy transfer) can be used to measure *trans* cleaving hammerhead ribozyme *in vitro* [20]. *Trans*-cleaving hammerhead ribozymes are used as gene silencing tools and can be designed *in silico* [18]. Similar to our proposed approach, this study uses fluorophore and quencher pair, but in their case , the fluorophore-quencher pair is directly attached to the ends of the RNA substrate or ribozyme of a *trans* cleaving HHR [20]. So, when their ribozyme self-cleaves, it separates the quencher from the fluorophore, resulting in fluorescence. Their approach differs from ours as it involves modifying the RNA molecule itself. Previous studies by [23] suggests that attaching a fluorophore and quencher *interferes* with thermodynamic stability of nucleic acid, which can impact the folding of RNA molecules and folding affects function.

1.8 Nucleic acid strand displacement reaction

Nucleic acid strand displacement reactions are major forces driving DNA nanotechnology [27]. A subfield of DNA nanotechnology, known as dynamic DNA nanotechnology, depends on the various reactions catalyzed by DNA, based on hybridization reactions [28]. Strand displacement reactions were used to develop cutting edge synthetic biology tools such as DNA polymerization motors [29], biosensors, amplifiers and digital and to run neural network like computations [30-32].

Single strand extension (toeholds) can be utilized to increase the rate of strand displacement and can be fine-tuned by varying the length, sequence and annealing temperature of the toehold [27, 33]. The displacement reaction starts with the invader strand binding to the toehold present on substrate strand at the 3′ end (Figure 4B). The invader strand initiates branch migration and will slowly displace the incumbent strand (Figure 4C). The rate of displacement in TMSDR is dependent on the GC content of the toehold as higher GC content allows the invader strand to bind strongly to the toehold and resist falling off [34].

The specificity of TMSDR lies in nucleic acid sequence dependency. Here, TMSDR are very sensitive to mismatched base pair making them highly specific compared to classical hybridization reactions [35]. This sensitivity to mismatches can be harnessed to detect specific nucleic acid strands in the environment. Researchers have demonstrated the use of TMSDR for enzyme free colorimetric detection of specific nucleic acid strands and for the detection of single nucleotide polymorphism in DNA strands [36, 37].Our approach is to detect the realistic concentration of cleaved-off detached RNA fragment generated from HHR strand scission reaction.
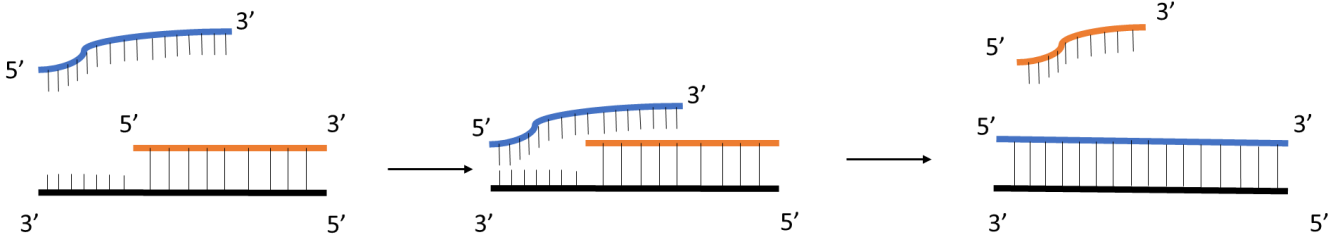
Figure 4. Toehold mediated strand displacement reaction.

(A) Incumbent strand (orange) binds to the substrate strand (black) leaving a single stranded domain (or toehold). Invader strand (blue) is also complementary to the substrate strand including the toehold. **(B)** Initiation of displacement by invader strand as it binds with the toehold. **(C)** Invader strand completely displaces incumbent strand.

1.9 Toehold mediated strand displacement to evaluate ribozyme cleavage

In contrast to the proceedings works, we designed and used a pre-annealed probe to detect RNA fragments cleaved-off an activated HHR. Figure 5 shows the probe-mediated kinetics measurement of a ribozyme. Figure 5 A shows the inactive ribozyme without the input DNA strand. This ribozyme does not cleave and remains inactive. Figure 5 B shows the incorporation of the input DNA oligo into the environment, which allows the ribozyme to fold into its native conformation and induces strand scission reaction. The smaller fragment (output strand) is released from the ribozyme as depicted in Figure 5 C. This output strand binds to the probe (Figure 5 D) via the toehold, which is present on the F-strand (Figure 5 E). It then displaces Q-strand via a strand displacement reaction, as shown in Figure 6 F. This separates the quencher from the fluorophore, allowing the Cy5 to fluoresce.
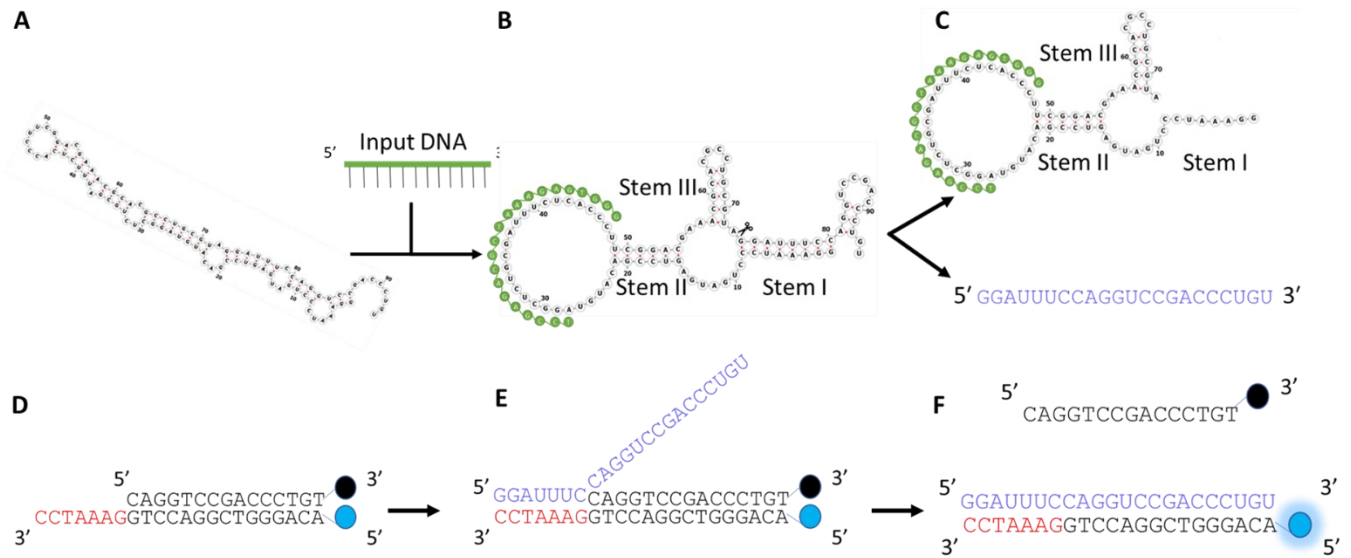
Figure 5. Schematic representation of the toehold mediated strand displacement reaction used in measuring the kinetics of hammerhead ribozyme cleavage reactions.

(A) Misfolded HHR in the absence of input DNA oligonucleotide. **(B)** The introduction of input DNA oligo (green strand) induces the formation of an active HHR core, culminating in cleavage activity. **(C)** Cleavage products: cleaved HHR bound with input and released output (blue strand) **(D)** and **(E)** Released output interacting with the toehold present on the pre-annealed probe; this interaction results in displacement of Q-strand (orange strand) **(F)** Displacement of the Q-strand results in the separation of the quencher from the fluorophore, culminating in detectable fluorescence.

1.10 Aim of the study and hypothesis

As mentioned previously, established methods to detect HHR cleavage involve radiolabelling of RNA molecules and analyzing cleavage products using denaturing polyacrylamide gels. This poses a problem as it separates all RNA strands by preventing hydrogen bond formation. We hypothesized that the output generated from HHR self-cleavage may remain attached with hydrogen bonds after cleavage or else the released output may re-attach to the cleaved HHR. Hence, the realistic concentration of output may be considerably lower than what is usually measured by gel.

Therefore, we propose and validate a new method to detect HHR cleavage without radiolabelling RNA molecule. We use TMSDR to evaluate HHR kinetics in real-time, devoid of radiolabelling. In addition, we determine the actual concentration of the cleaved-off RNA fragments using radiolabelling approach and TMSDR.

The objectives of this thesis are:

- Objective 1: To develop a fluorescent probe that can be utilized to measure HHR cleavage in real time without modifying or labeling RNA molecule.

- Objective 2: To increase the concentration of output strand by developing doubler HHRs, that increase by a factor >1 the amount of output, upon induction by one input strand.

The remainder of the thesis will demonstrate that we have achieved objective 1. As to objective 2, we were successful in designing active doubler (and converter) hammerhead ribozymes. However, their performance leaves a lot for future work.

Chapter 2 Experimental Design of Probe and Inducible Hammerhead Ribozymes

2.1 Probe design

A probe comprised of two ssDNA, one labelled with quencher (Black hole quencher-3) and another labelled with fluorophore (Cy-5). The fluorophore labelled strand, also called 'F-strand', was labelled with Cy-5 fluorophore (Abs. 647nm, ex. 665nm). The optimum excitation and emission wavelengths were optimized in Tecan M1000 pro by the 3D scanning command. The quencher labelled strand, termed as 'Q-strand', was labelled with black hole quencher -3 (BHQ-3). The F-strand is longer than the Q-strand by seven nucleotides to create an overhang at the 3′ end of the F-strand. This single stranded segment of the probe will be used as a toehold (Figure 6). The probe was designed so the melting temperature of Q-strand is above 40°C and the length of the toehold is greater than 4 nucleotides. The length of the toehold has impact on TMSDR, as less than four nucleotides decreases the rate of the displacement reaction [27, 34]. To ensure displacement, the toehold length was set to be 7 nucleotides. Melting temperature of probe was set to greater than 40°C to make the probe stable at 37°C, ensuring fluorophore quenching. Other criteria were to evaluate the invading strand and its folding. Pre-annealed probe provides a target (the toehold) for the invading strand and hence, the invading strand should not base pair with itself to prevent interaction with the toehold present on the F-strand.
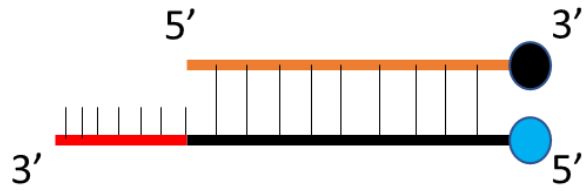
Figure 6. Schematic diagram of probe

The red segment highlights the seven nucleotides toehold sequence. The black circle represents the

black hole quencher molecule on the Q-strand (orange), while the blue circle represents fluorophore

Cy-5 on the F-strand (in red and black).

2.2 Computational design of inducible hammerhead ribozyme sequences

The computational algorithm that is presented in this thesis is an extension design and implemented by Kamel [38], which itself is based on the algorithm used by [17]. The key difference in our algorithm is instead of a random search, it employs an *evolutionary algorithm* (EA) to search for inducible hammerhead ribozyme strands. An EA is a method of search and optimization which simulates evolution in computational environment. EA operates on a population of candidate solutions (*individuals*) to a problem. The individuals have certain criteria that restricts the form of solution. At the start, all individuals are randomized. Then the fitness of all the individuals are evaluated. The fitness is a measure of how well an individual is close to solve the problem and hence we seek the individual with maximum fitness. Individuals that are selected are called parents. These individuals are mutated, and the resulting solutions are termed as *offspring*. To maintain the population size, the parents and offspring are selected by *survivor selection.* The algorithm is cycled through this process several times to generate the best solution to the problem.

This algorithm is represented by the ribonucleotide bases as described in the Table 2. There are three parts of this algorithm: *evolvable, constant,* and *dependent.* The evolvable segments can be randomized and there are no constrains on that. Constant segments, as the name suggests are specified by the user prior to mutations and are not changed throughout the whole operation. The dependent segments are generated by taking the reverse complement of their corresponding *parent segment*. This consist of copying that parent segment, reversing it, and changing every A to U, U to A, G to C, and C to G. Table 2 contains all 15 segments that are used to generate the inducible HHR RNA strand. First 14 segments are part of the inducible ribozyme and 15th segment is the input strand that induces the ribozyme.

RNA folding consists of predicting RNA secondary structure using software. We used the ViennaRNA software package [39] for folding generated RNA strands. An RNA strand is folded twice, in *ON* state and *OFF* state. In off state, RNA strand is folded without any constraint but in ON state, it was folded with following constrains:

........................xxxxxxxxxxxxxxxxxxxxxx...

These dots and the "x" represent all the bases of the RNA strand. If the character is a dot, there is no constraint on that base, but if the character is "x", then the base is forced to be unpaired during folding. The constraint forces the input binding site to remain unpaired during ON state. This stimulates binding of the input strand to this site and makes that segment unavailable to bind with any other site of the ribozyme. Folding also gives information about *minimum free energy (MFE)* of the RNA structure, meaning that is the predicted most prominent structure in which the RNA will fold, and *ensemble diversity* (a measurement of how many different structures a strand will sample), for a total of four different outputs.

From folding results, three fitness values are calculated. The *ON score* is the negative of the number of core and stem bases that are incorrectly paired in the ON state. The *OFF score* is the number of core and stem basses that are incorrectly paired in OFF state. The *diversity score* is the negative of the average of the ensemble diversity of the two states. A low ensemble diversity is desired, since this implies that the MFE structure is representative of the statistical ensemble of secondary structures.

Tournament selection is used to select the parents. Each parent is the winner of a tournament. For a population size N, N parents are selected, meaning that N tournaments are performed. Each tournament consists of k individuals competing against each other. These individuals are selected randomly from the population. The winner of a tournament is determined by sorting the

participants by their fitness values. Since each individual has three different fitness values, they are sorted into a set of non-dominated fronts. An individual A is said to dominate another individual B if all three of A's fitness values are higher than individual B's. Each member of the same non-dominated front is dominated by an equal number of individuals. The members of the first non-dominated front are dominated by no other individuals. The tournament winner is randomly selected from the first non-dominated front. The set of non-dominated fronts is obtained using the NSGA-ii algorithm [40].

All the parents are copied into offspring set and are mutated M times, where M is mutation rate. Then parents and offspring are merged into a set of 2N individuals. NSGA-II algorithm was used to sort the set and N individuals with the lowest domination counts are selected as survivors. The survivors act as the new population in the next generation.

2.3 Pseudocode of the algorithm

```
// The initial generation

Randomly initialize a population of N individuals

For each individual in the population

Generate the dependent segments

Concatenate all segments into the inducible HHR (converter) and
input strands

Fold the converter strand with and without constraints

Calculate the ON, OFF, and diversity scores
```

```
//The remaining generations

For each of the remaining G-1 generations

     Select N parents from the population

     Produce N offspring through mutation

For each offspring individual

Generate the dependent segments

Concatenate all segments into the converter and input strands

Fold the converter strand with and without constraints

Calculate the ON, OFF, and diversity scores

Select N survivors from the union of the parents and offspring.

Mark the survivors as the new population
```

Population (N)	300
Number of generations (G)	200
Tournament size (k)	20
Mutation rate (M)	4

Table 1. EA parameters

Name	Type	Length	Strand Id	Position in strand	Fixed Sequence	Parent segment
Stem 1 A	Evolvable	8	0	0	N/A	N/A
Core A	Constant	8	0	1	CUGAUGA G	N/A
Stem 2 A	Evolvable	5	0	2	N/A	N/A
Pre OBS	Evolvable	4	0	3	N/A	N/A
OBS	Evolvable	22	0	4	N/A	N/A
Post OBS	Evolvable	1	0	5	N/A	N/A
Stem 2 B	Dependent	5	0	6	N/A	Stem 2 A
Core B	Constant	5	0	7	CGAAA	N/A
Stem 3 A	Evolvable	4	0	8	N/A	N/A
Stem 3 Hp	Evolvable	4	0	9	N/A	N/A
Stem 3 B	Dependent	4	0	10	N/A	Stem 3 A
Core C	Constant	2	0	11	UA	N/A
Stem 1 B	Dependent	8	0	12	N/A	Stem 1 A
Overhang	Evolvable	14	0	13	N/A	N/A
Input	Dependent	22	1	0	N/A	OBS

Table 2. Segments of EA used to generate inducible ribozyme and input strand.

OBS= oligo binding site, N/A = Not applicable

Chapter 3 Experimental Methods

3.1 PCR assembly of converters and doublers

Overlapping oligodeoxynucleotides (Figure 7, Table 3 and Table 4) were designed with Primerize [41] and were assembled by PCR (Bio-Rad T100) using Primers F1, R1, F2 and R2 (Figure 7). The PCR reaction was carried out in a fixed volume of 100 µl, containing primers F1 (2 µM), R1 (0.2 µM), F2 (0.2 µM), R2 (2 µM), Taq polymerase (hotStar Taq Plus from QIAGEN) with its reaction buffer at 1x, Q-solution (1x from QIAGEN), 0.2 mM of dNTPs (DGel electrosystem) and milli-Q water. The reaction mixture was subjected to 15 min denaturation at 95°C and 15 cycles consisting of: 30 s denaturation at 95°C, 30 s annealing at 50°C and 30 s extension at 72°C. PCR was validated by visualizing 5 µl of reaction mixture on 2% agarose gel containing gel red (Trans). The remaining PCR product was ethanol precipitated.
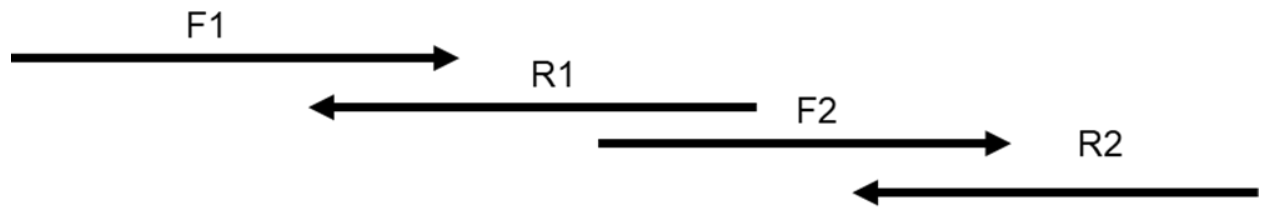
Figure 7. Schematic representation of *Primerize* assembly design [41]

Converter 1	F1	5'TTCTAATACGACTCACTATAGGAGTTCCCTGAT 3'
	R1	5'GCGGTGACAAGACTGGACCTATTAGCCACTCTCATCAGGGAACTCCTATAGTGAGTCGT 3'
	F2	5'CCAGTCTTGTCACCGCCACCACTCGAAATTCAAGGGTGAATAGGAACTCCGAGAGCA 3'
	R2	5'TTACATTTGCTCTCGGAGTTCCTATTCACCCTT 3'
	Input	5'GGCGGTGACAAGACTGGACCTA 3'
Converter 2 (Ribozyme)	F1	5'TTCTAATACGACTCACTATAGGAAATCCCTGATGAGTCCGACATGTAGGCT 3'
	R1	5'CGTCCGAAGGGTGAGAAATCGCAGAGCCTACATGTCGGACTCAT 3'
	F2	5'TCTCACCCTTCGGACGAAACGCACGCCTGCGTAGGATTTCCA 3'
	R2	5'ACAGGGTCGGACCTGGAAATCCTACGCAGGCGTGCGTT 3'
	Input	5'GGGTGAGAAATCGCAGAGCCTA
Converter 3	F1	5'TTCTAATACGACTCACTATAGGCATTCCCTG 3'
	R1	5'CGGCTCACAAAACTATAGACCTAATGATATCTCTCATCAGGGAATGCCTATAGTGAGT 3'
	F2	5'GGTCTATAGTTTTGTGAGCCGTATCTCGAAACTTGTAGGCAAGTAGGAATGCCA 3'
	R2	5'GGACGACCCTTTGTGGCATTCCTACTTGCCTACA 3'
	Input	5'GGCTCACAAAACTATAGACCTA 3'
Converter 4	F1	5'TTCTAATACGACTCACTATAGGATTTCCCTGATGAGAGGCCATCGTAG 3'
	R1	5'AGGCCCGGCGTTTAAGAAACCGGACCTACGATGGCCTCTCATCA 3'
	F2	5'ACGCCGGGCCTCGAAAGTAATAAGTTACTAGGAAATCCGCCAGT 3'
	R2	5'CATCTTTCACTGGCGGATTTCCTAGTAACTTAT 3'
	Input	5'GGCGTTTAAGAAACCGGACCTA 3'
Converter- 2 +2 bp (Ribozyme+ 2bp)	F1	5'TTCTAATACGACTCACTATACTGGAAATCCCTGATGAGTCCGACATGTAGGCT 3'
	R1	5'CGTCCGAAGGGTGAGAAATCGCAGAGCCTACATGTCGGACTCAT 3'
	F2	5'TCTCACCCTTCGGACGAAACGCACGCCTGCGTAGGA 3'
	R2	5'ACAGGGTCGGACCTGGAAATCCTACGCAGGCGTGCGTT 3'
Converter 2 + 14 bp	F1	5'TTCTAATACGACTCACTATAACAGGGTCGGACCCTGGAAATCCCTGATGAGTCCGACA 3'

(Ribozyme+ 14bp)	R1	5'TGAGAAATCGCAGAGCCTACATGTCGGACTCATCAGGGA 3'
	F2	5'AGGCTCTGCGATTTCTCACCCTTCGGACGAAACGCAC 3'
	R2	5'ACAGGGTCGGACCTGGAAATCCTACGCAGGCGTGCGTTTCGTCCGAAG 3'

Table 3. *Primerized* converter sequences

All converter sequences has T7 promoter in F1 followed by GG [41].

Doubler 1	F1	5'TTCTAATACGACTCACTATAGGTCCCCGCCCTGATGAGCCTCAAGGTTTACATTTGC 3'
	R1	5'GGGCGGGGACCTTTCGCCTCAGGGAACTCCGAGAGCAAATGTAAACCTTGAGGCTC 3'
	F2	5'AGGTCCCCGCCCTGATGAGCCAGCCTGGGCTGGCGAAAAGAGGTAAGCCTCTTAGGCG 3'
	R2	5'TAGGTCCAGTCTTGTCACCGCCTAGGTCCAGTCTTGTCACCGCCTAAGAGGCTTACCT 3'
	Input	5'GGAACTCCGAGAGCAAATGTAA 3'
Doubler 2	F1	5'TTCTAATACGACTCACTATAGGCTCCACCCCTGATGAGGTCCCGCTCACA 3'
	R1	5'CAGGGGTGGAGCCTTTCGGTCCCAGGATTTCCAGGTCCGACCCTGTGAGCGGGACCTC 3'
	F2	5'AGGCTCCACCCCTGATGAGAACGGCATACCGTTCGAAACCCTAGTATTAGGGTAGGGT 3'
	R2	5'TAGGCTCTGCGATTTCTCACCCTAGGCTCTGCGATTTCTCACCCTACCCTAATACTAGGGTT 3'
	Input	5'GGATTTCCAGGTCCGACCCTGT 3'
Doubler 3	F1	5'TTCTAATACGACTCACTATAGGTCTGAGCCCTGATGAGCTGGGCTGTGGACGACCCTTTG 3'
	R1	5'GGCTCAGACCTTTCGCTGGGGGGAATGCCACAAAGGGTCGTCCACAG 3'
	F2	5'GCGAAAGGTCTGAGCCCTGATGAGTGGGGAAATCCCCACGAAACGGGTACTGACCCGTAG 3'
	R2	5'TAGGTCTATAGTTTTGTGAGCCTAGGTCTATAGTTTTGTGAGCCTACGGGTCAGTACCCG 3'
	Input	5'GGAATGCCACAAAGGGTCGTCC 3'
Doubler 4	F1	5'TTCTAATACGACTCACTATAGGTCCACGCCCTGATGAGAAAGTACCTCATCTTTCACTGG 3'
	R1	5'AGGGCGTGGACCTTTCGAAAGTGGGAAATCCGCCAGTGAAAGATGAGGTACTTTCT 3'
	F2	5'AAGGTCCACGCCCTGATGAGAAGGGGATCCCCTTCGAAACCCCGCGACCGGGGTAG 3'
	R2	5'TAGGTCCGGTTTCTTAAACGCCTAGGTCCGGTTTCTTAAACGCCTACCCCGGTCGCG 3'
	Input	5'GGAAATCCGCCAGTGAAAGATG 3'
	F1	5'TTCTAATACGACTCACTATAATCGCGGCGCGTAGAATCATCCTGTGATTCCTGATGAGTT 3'

D1 doubler	R1	5'CGCGGCGCGTTTCGTTTCCATTGATTCCTGTGGAAACTCATCAGGAATCACAGGAT 3'
	F2	5'ACGCGCCGCGATAAAAAAAAAAAAGCGCCGCGATCTGATGAGAAAGGTTTGATTCACCTTTCG AACCTTAGTGT 3'
	R2	5'TACGCGCCGCGATTACCTTAGTAGGACACTAAGGTTTCGAAAGGTGAATCAAA 3'
	Input	5'GTCCTTAGTT 3'

Table 4. *Primerized* doubler sequences

All doubler sequences has T7 promoter followed by GG (Except D1) [41].

3.2 In vitro transcription and RNA purification

In vitro RNA synthesis was performed as previously described [11], with slight modifications. When larger quantities were required, reaction was carried out in a fixed volume of 1 ml. The reaction mixture contained 80 mM HEPES (pH 7.5), 24 mM $MgCl_2$, 40 mM dithiothreitol, 2 mM spermidine, 6 µg/ml T7 polymerase, 150 µl of PCR product (for 1ml transcription, 10 PCR reactions (100 µl each) were pooled together, precipitated and resuspended in 150 µl milli-Q water), 2 mM rNTPs, 1x pyrophosphatase (Roche diagnostics) and 200 U (40 U/µl) RiboLock (Thermo Fisher Scientific). The reaction mixture was incubated at 37°C for 150 minutes, treated with 10 U of DNase (New England Biolabs), incubated at 37°C for 30 minutes. The RNA was extracted with phenol-chloroform, and the aqueous phase was ethanol precipitated. The RNA was purified in 10 % denaturing (8 M urea) polyacrylamide gel. The gel was revealed by UV-shadowing. The band of interest (highest band on gel, as there was some level of cleavage during transcription) was excised and eluted in 0.3 M NaCl overnight at 4°C. The eluent was ethanol precipitated and resuspended in nuclease free water.

3.3 Radiolabeling of ribozyme using [α-^{32}P] UTP during transcription

Radiolabeling of RNA was conducted as previously described with minute modifications. Here, the reaction mixture consisted of 1X transcription buffer (see above), 15 µl of PCR product (100 µl PCR reaction ethanol precipitated and resuspended in 20 µl milliQ water), 2 mM of GTP, CTP, ATP, 0.125 mM UTP, 1x pyrophosphatase (Roche diagnostics) and 40 U RiboLock (Thermo Fisher Scientific) and 1 µl of [α-^{32}P] UTP (Perkin Elmer) per 50 µl reaction. The reaction mixture was ethanol precipitated and analyzed in 10% denaturing polyacrylamide gel (For original doubler transcripts, ethanol precipitated reaction mixture was isolated on native 10% gel prepared in TBMg); the product was revealed by phosphorimaging (Typhoon 9500 FLA; GE Healthcare Life Sciences). The band of interest was resected and eluted in 0.3 M NaCl overnight at 4°C. The eluent was ethanol precipitated and resuspended in nuclease free water.

3.4 Purification of doubler molecule on native gel

Radiolabeled transcription was performed as describe above. The samples were purified on 10% native polyacrylamide gel prepared in TBMg. Loading buffer was also prepared in TBMg (5x). The gel purification was conducted at 4°C to prevent the detachment of 44 nucleotide strand generated as a result of constitutively active second ribozyme in doubler (Figure 12 A).

3.5 Preparation of fluorescent probe

Oligodeoxynucleotides were conjugated at the 5' end with Cy5 and at the 3′ end with Black hole quencher (Alpha DNA, Montreal, Canada). The strand with the Cy-5 at the 5′ end was named the 'F-strand' (5′-ACAGGGTCGGACCTGGAAATCC-3′) while the strand with the Black hole quencher-3 (BHQ-3) at 3′ end was called the 'Q-strand' (5′- CAGGTCCGACCCTGT-3′) (Figure 6). The probe was prepared in cleavage buffer (100mM NaCl, 50mM tris-HCl pH 7.5, 25mM KCl) with 0.5 µM F-strand and 0.6 µM Q-strand per 10µl reaction. The reaction was incubated in

thermocycler (Bio-Rad T100) 3 min denaturation at 95°C, 15 min annealing at 50°C and 15 min annealing at 37°C).

3.6 Calibration of probe and standard curve generation

The prepared probe was calibrated using ss-DNA oligonucleotide mimicking the ribozyme output (5′-GGATTTCCAGGTCCGACCCTGT-3′) (Figure 10 B). We called this strand the 'D-strand' (Displacer DNA-strand). Different concentrations of D-strand, ranging from 0.05 μM to 2 μM were mixed with 0.5μM pre-annealed probe. The reaction mixture was incubated at 37°C and analyzed using a fluorescent plate reader (Tecan M1000 pro) at 647 nm excitation and 665 nm emission. The probe was also calibrated using DNA displacer strand called 'D-strand'. Comparison of R-strand and D-strand standard curve is illustrated in Figure 26.

3.7 Analysis of Hammerhead ribozyme kinetics on polyacrylamide gel

Ribozyme kinetics were assayed using a prelabeled [α-^{32}P] UTP ribozyme. The reaction was performed in a fixed volume of 10μl, containing 100mM NaCl, 50mM Tris-HCl pH-7.5, 25mM KCl, 10 mM MgCl$_2$, 10 μM input oligodeoxynucleotide (Figure 9 B) and 1 μl of the labelled ribozyme. The reaction was started by adding MgCl$_2$. The reaction was incubated at 37°C. Sequentially, the aliquots of reactions reaction were stopped at 30 minutes intervals using denaturation buffer (80 % formamide, 0.5 mM EDTA, 0.02% bromophenol blue and 0.02% xylene cyanole). The samples were analyzed on 10% denaturing polyacrylamide gel, the gel developed by phosphorimaging and the band intensity was determined using ImageQuant software (GE Healthcare Life Sciences). The cleavage of ribozyme was determined as a percentage ratio of cleaved fragments (Cleaved HHR + output - background) and all HHR (Cleaved HHR + output + uncleaved HHR - background).

3.8 Analysis of hammerhead ribozyme kinetics with strand displacement

A pre -annealed probe was used to evaluate HHR cleavage kinetics. Here, 0.5 µM of a pre-annealed probe was mixed with 10 mM $MgCl_2$, 10 µM input oligodeoxynucleotide and 1 µM ribozyme per 10 µl reaction. The reaction mixture was incubated at 37°C. The fluorescence emitted was measured using a fluorescent plate reader. (Tecan M1000 Pro) Readings were taken every 30 minutes.

Chapter 4 Experimental Results

4.1 Hammerhead ribozyme cleavage assay (Converters)

The *in vitro* cleavage of all designed HHRs (Converters) in the presence of their input oligonucleotides was performed in 100mM NaCl, 50mM Tris-HCl (pH-7.5), 25mM KCl, and 10mM $MgCl_2$ and 10µM input DNA oligonucleotide. All the experiments were conducted at 37°C and the incubations were performed in a Bio-RAD T100 thermal cycler to prevent condensation on the lid of the microfuge tubes. Different conditions were used to assess the inducibility of the converter HHR (YES gate) in the presence and in the absence of input. Figure 8 displays the kinetics of converters 1, 2 and 3. Three timepoints were taken at 1h, 2h and 24h. From the gel, it is clear that all converters cleave in the presence of 10mM $MgCl_2$ and in the presence of the input DNA oligo. All converter sequences are shown in Table 5.

Converter 1	5'GGAGUUCCCUGAUGAGAGUGGCUAAUAGGUCCAGUCUUGUCACCGCCACCACUCGAAAUUCA AGGGUGAAUAGGAACUCCGAGAGCAAAUGUAA 3'
Converter 2 (Ribozyme)	5'GGAAAUCCCUGAUGAGUCCGACAUGUAGGCUCUGCGAUUUCUCACCCUUCG GACGAAACGCA GCCUGCGUAGGAUUUCCAGGUCCGACCCUGU 3'
Converter 3	5'GGCAUUCCCUGAUGAGAGAUAUCAUUAGGUCUAUAGUUUUGUGAGCCGUAU CUCGAAACUUGUAGGCAAGUAGGAAUGCCACAAAGGGUCGUCC 3'
Converter 4	5'GGAUUUCCCUGAUGAGAGGCCAUCGUAGGUCCGGUUUCUUAAACGCCGGGC CUCGAAAGUAAUAAGUUACUAGGAAAUCCGCCAGUGAAAGAUG 3'
Converter 2 +2bp	5'CUGGAAAUCCCUGAUGAGUCCGACAUGUAGGCUCUGCGAUUUCUCACCCUU CGGACGAAACGCACGCCUGCGUAGGAUUUCCAGGUCCGACCCUGU 3'

(Ribozyme +2bp)	
Converter 2 +14bp (Ribozyme +14bp)	5'ACAGGGUCGGACCCUGGAAAUCCCUGAUGAGUCCGACAUGUAGGCUCUGCG AUUUCUCACCCUUCGGACGAAACGCACGCCUGCGUAGGAUUUCCAGGUCCGAC CCUGU 3'

Table 5. Converter sequences

Self-cleavage of the 94 nucleotides long ribozymes culminates in two fragments: a 72 nucleotides cleaved ribozyme and a 22 nucleotides output strand. The expected lengths of the RNA molecules are noted on the left side of the gel. Bromophenol blue and xylene cyanole dyes were used as size markers. These results confirm that converters 1, 2 and 3 indeed work as YES logic gates, cleaving only in the presence of input and $MgCl_2$ after 1h and 2h. However, after 24 hours, all tested ribozymes cleave without input in the presence of Mg^{2+}. An additional assay was performed using converter-2 to investigate the effect of input concentration on cleavage efficiency (Appendix Figure 25). Confusion matrix for converter-2 was also performed using 4 mutant inputs (Table 6 and appendix Figure 27). All band intensities were revealed and quantified using photostimulated luminescence, also known as phosphorimaging.

Mutant input 1	5'GCGTGAGAAATCGCAGAGCCTA 3'
Mutant input 2	5'GGGTGAGAAATCGCAGAGCGTA 3'
Mutant input 3	5'GCGTGAGAAATCGCAGAGCGTA 3'
Mutant input 4	5'GCGTGAGAAACGCAGAGCGTA 3'
Original input	5'GGGTGAGAAATCGCAGAGCCTA 3'

Table 6. Converter 2 mutant inputs.

Changed nucleotides are highlighted.

It would appear that one mutation is tolerated for these 22 nucleotides inputs, but two or more mutations seem to completely abolish activating capability of input sequences (Figure 27).
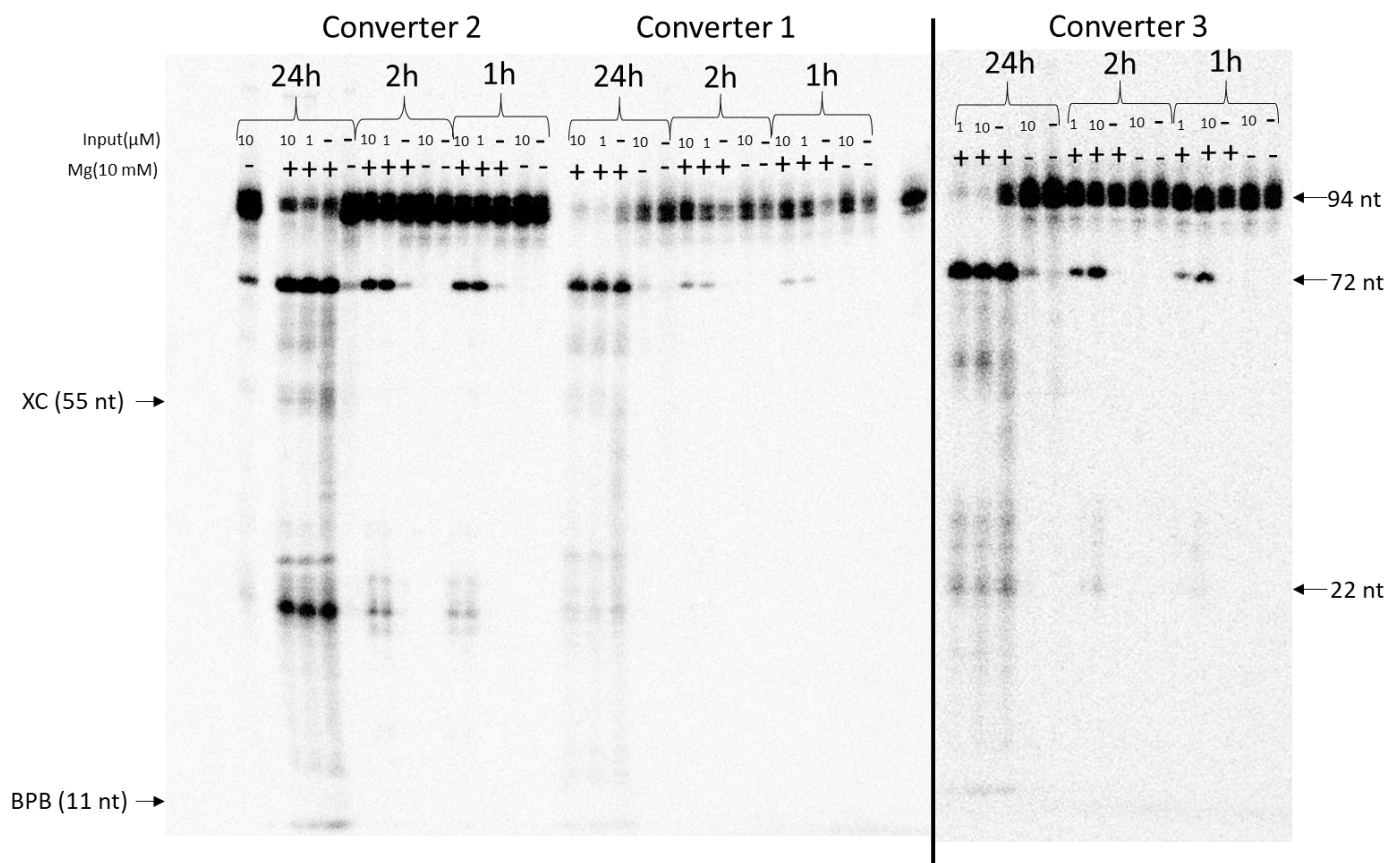
Figure 8. Converter HHRs 1, 2 and 3 cleavage assays

Converter 1, 2 and 3 were labelled during transcription with [α-^{32}P] UTP and were incubated in 100 mM NaCl, 50 mM Tris-HCl (pH 7.5) and 25 mM KCl, and in the presence or absence of input or MgCl$_2$. Lanes are as indicated in the figure: all lanes contain ribozyme; either without (negative control) or with 10 mM MgCl$_2$; and either without input or with 1 or 10 µM (as indicated). All samples were loaded on 10% denaturing 8M urea polyacrylamide gel. XC (xylene cyanol) and BPB (bromophenol blue) appear as 55 nucleotides fragment and 11 nucleotides fragment, respectively. Corresponding fragment sizes are shown on the right side of the gel.

4.2 Kinetics of Converter 2 and Converter 2 + 2bp and Converter 2 + 14bp

Converter 2 was characterized by performing kinetics over 30 min intervals for a period of 180 minutes. All HHRs (Figure 9 A, B and C) kinetics were assayed using prelabeled [α-^{32}P] UTP ribozymes. Aliquots were taken, reaction stopped at 30-minute intervals using denaturation buffer, and the products were analyzed on a 10 % denaturing polyacrylamide gel (Figure 9 D), as described in the materials and methods section (Section 3.7). As expected, an increase in cleavage over time was noticed (Figure 9 D). These results confirm the previous results that converter 2 works as a YES logic gate in the presence of input and MgCl$_2$. These results also confirm that the Converter-2 + 2 bp and Converter-2 + 14 bp cleave in the presence of MgCl$_2$ and input DNA oligonucleotide.
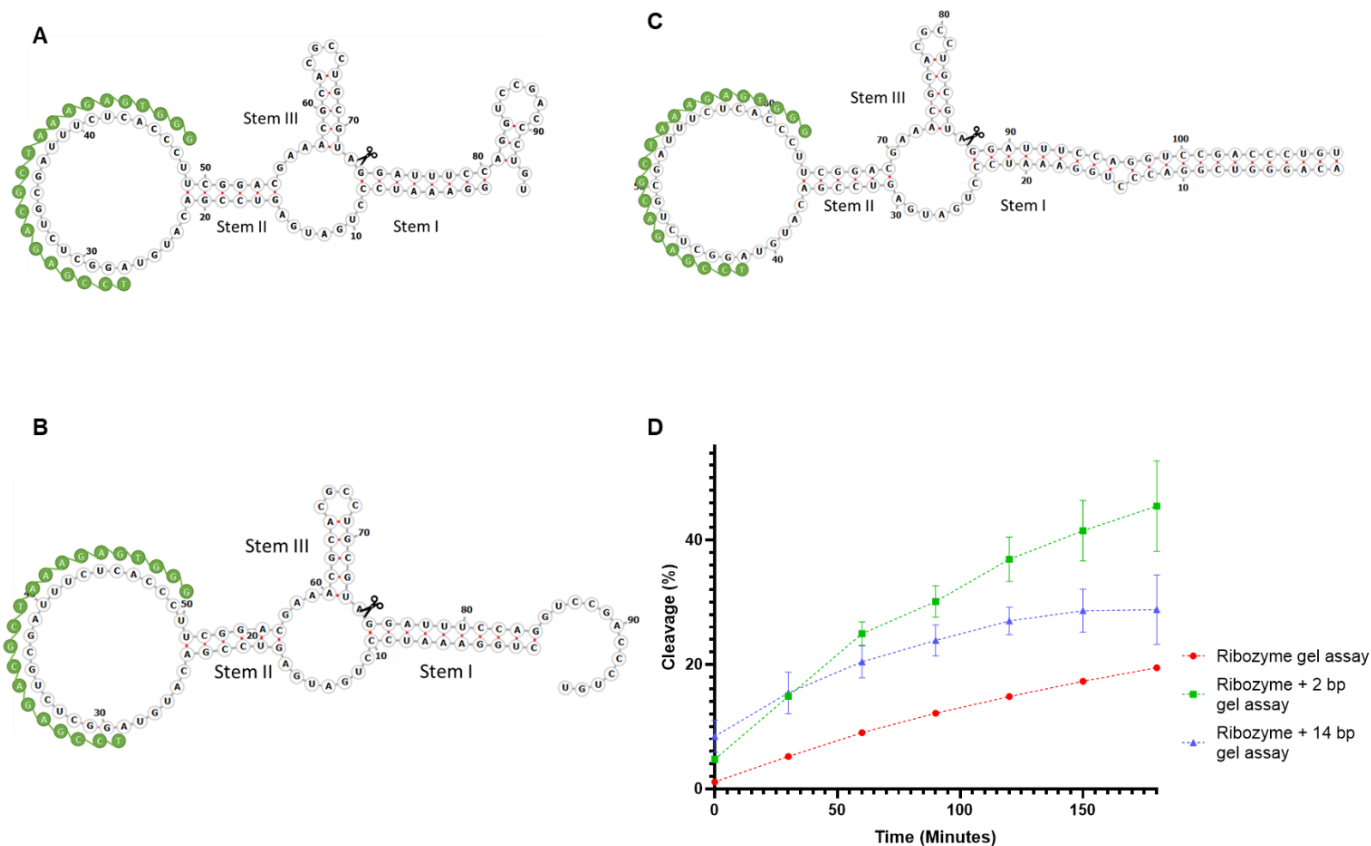
Figure 9. Converter 2 (Ribozyme), Converter-2 + 2 bp (Ribozyme + 2 bp) and Converter-2 + 14

bp (Ribozyme + 14 bp) kinetics using [α-^{32}P] UTP labelling.

Standard cleavage buffer conditions were used, and all the reactions were carried out at 37°C.

(A) Ribozyme binding with input DNA oligonucleotide (green strand) (5′

GGGTGAGAAATCGCAGAGCCTA 3′) [42] **(B)** Ribozyme+2bp binding with input DNA

oligonucleotide (Same input sequence as Ribozyme) **(C)** Ribozyme+14bp binding with input

DNA oligonucleotide (Same input sequence as Ribozyme) **(D)** Graphical representation of

cleavage over time for 180 minutes (Triplicates).

4.3 Evaluation of HHR kinetics by strand displacement reaction using a fluorescent probe

The assessment of HHR kinetics using radiolabeling suffers from certain limitations. For example, determining the concentrations of cleaved ribozymes and cleaved detached RNA outputs using denaturing gels is problematic. This is because a gel shows all output strands of equal length in the same band, whether these strands have actually detached from the rest of the ribozyme or not, post cleavage. In addition, this method is time consuming and involves the use of radioisotopes, which are carcinogenic [43]. To overcome these limitations, we sought to evaluate HHR kinetics using predesigned fluorescent probes.

Interestingly, we noticed (Figure 10A) an increase in fluorescence intensity with time in the assay group (HHR with input and Mg^{2+}). However, little or no change in fluorescence intensity was noticed in either the background group or the HHR alone group (Figure 10A). Interestingly, for both Ribozyme+2bp and Ribozyme+14bp assay groups, the observed fluorescence was near background levels. Taken together, these results provide evidence that the cleaved output from the original ribozyme binds to the toehold, displaces the Q-strand, leading to the observed fluorescence.

Furthermore, to determine the concentration of HHR output, we generated a standard curve using an R-strand equivalent to the output strand (Figure 10B). Different concentrations of R-strands were mixed in with the probe and assayed using a fluorescent plate reader. We observed a stoichiometric relationship between R-strand concentration and fluorescence (Figure 10B). These results demonstrate an increase in TMSDR fluorescence as a function of increased R-strand concentration. Thus, the generated standard curve can be utilized to interpolate the fluorescence values obtained from the TMSDR assay and hence, determine the concentration of detached output strand, generated by ribozyme self-cleavage.

Interpolated values were plotted for all three ribozymes. The original ribozyme shows the highest activity level (as determined by TMSDR) relative to Ribozyme+2bp and Ribozyme+14bp (Figure 10C). The original ribozyme has only 8 base pairs in stem I joining the output strand to its complementary strand (Figure 1). Two larger ribozymes were generated: a ribozyme with 10 base pairs in stem I (Ribozyme+2bp) and another ribozyme with 22 base pairs in stem I (Ribozyme+14bp) (Figure 9B and C). The TMSDR results (Figure 10A, further highlighted in Appendix Figure 24) show a decrease in fluorescence as a function of increased base-pairing with the output strand.
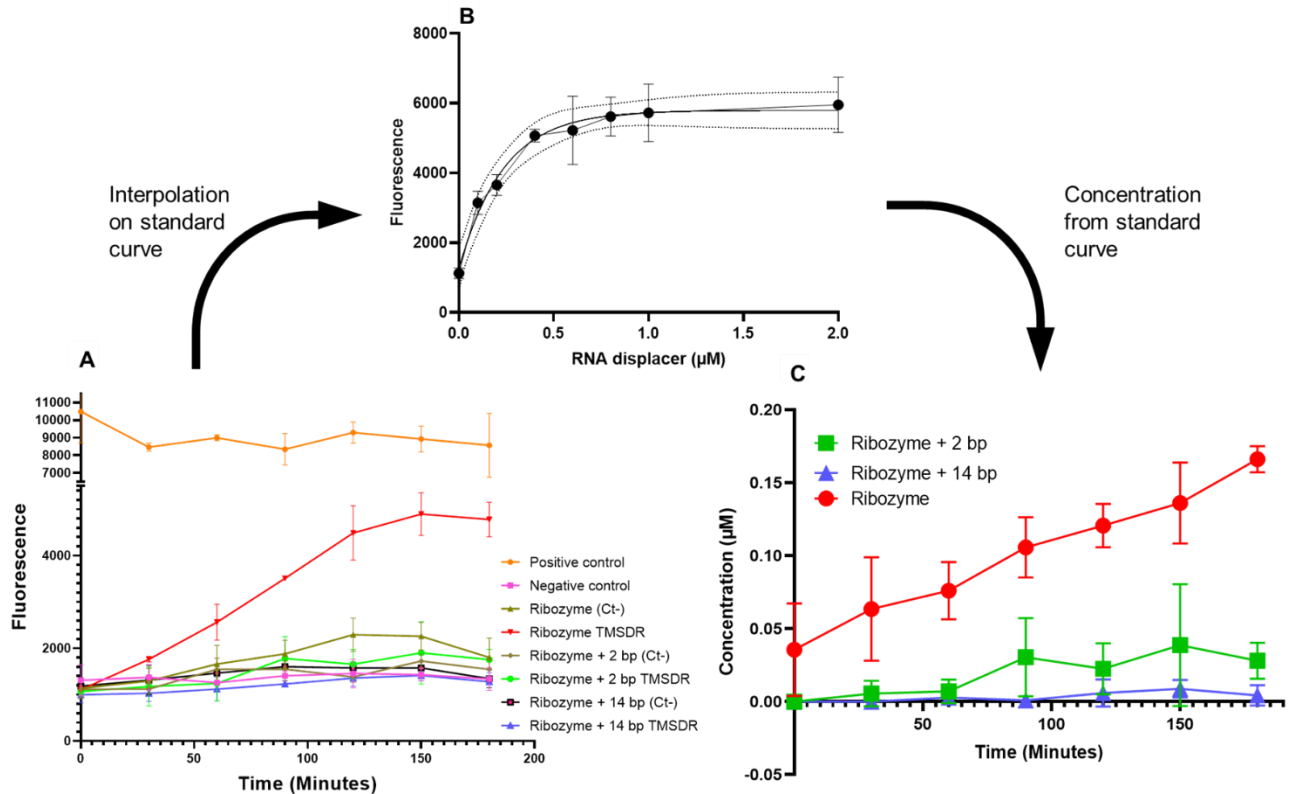
Figure 10. Analysis of the YES gates using fluorescent probe and TMSDR

Analysis of the YES gate using probe (with Cy-5 as fluorophore and Black hole quencher as quencher). **(A)** 0.5μM of probe and 1 μM of ribozyme were used in the assay. 10 μM of the R-strand with the probe was used as positive control, and a quenched probe was used as negative control. Ribozyme without Mg^{2+} and without input DNA was used as another negative control (Ct). The assay group includes 10 μM input DNA, 10 mM Mg^{2+}. Readings were taken every 30 minutes over a period of 180 minutes. The same protocol was followed for Ribozyme+2bp and for Ribozyme+14bp. **(B)** The standard curve for the 0.5 μM probe using the same reagents as for the assay. Different concentrations of the RNA displacer strand were used (0.05, 0.1, 0.2, 0.4, 0.6, 0.8, 1 and 2 μM). **(C)** Fluorescence values were interpolated on RNA standard curve to determine the concentration of released output strand from all assayed ribozymes.

Comparison of HHR cleavage in conventional (gel) versus TMSDR

To better evaluate the output concentration derived from the conventional approach (gel) and the new probe approach (TMSDR), we compared cleavage activity measured by gel band intensity with cleavage activity as reflected by probe fluorescence (Figure 11A). These results indicated that the two approaches measure the progress of cleavage reactions in different ways and provide complementary information: breakage of the phosphodiester linkage at the cleavage site measured with the denaturing gel vs. amount of dissociated products measured by TMSDR.

As demonstrated in Figure 11B, the cleavage from the gel is comparable with cleavage derived from the TMSDR assay in case of original ribozyme (normalized). However, as the base pairing with the output strand increases, even by as little as 2nt, the amount of released output decreases considerably, as illustrated by the green bars representing ribozyme+2bp. In case of ribozyme+14bp, virtually no cleavage activity was observed from TMSDR as compared to its gel counterpart. It is important that the experimenters understand that and hence, utilizes the method most appropriate to the particular needs of their own projects.
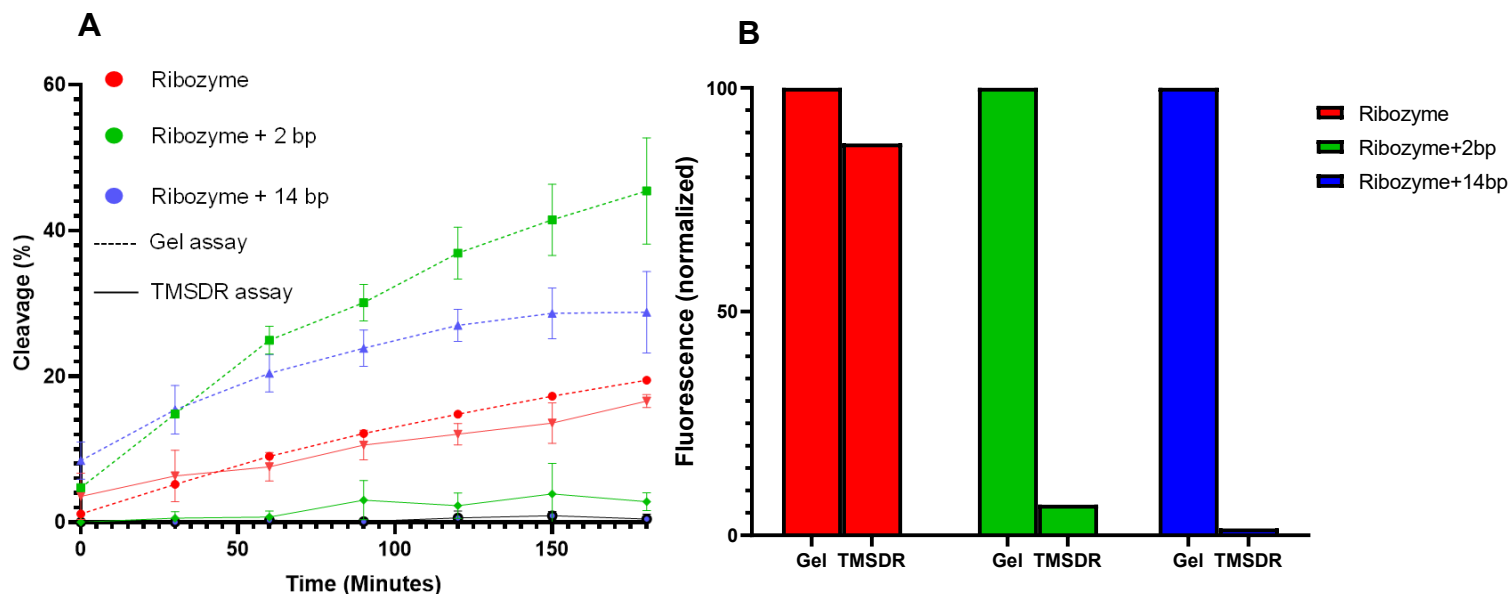
Figure 11. TMSDR vs. Gel cleavage analysis

(A) Comparison of cleavage obtained from [α- ^{32}P] UTP labelled ribozymes (dotted lines) and TMSDR (solid lines). **(B)** The area under the curve, representing total emitted fluorescence (normalized), was calculated from the graph for the original Ribozyme, Ribozyme+2bp and Ribozyme+14bp.

4.4 Kinetics of doublers

From previous experiments with TMSDR (Figure 11), the actual concentration of a detached output strand is lower than cleavage and it depends on the base pairing between the output strand and ribozyme. Hence, we developed a new molecule, a doubler, to increase the output strand's concentration in the environment by providing two outputs instead of one. We propose several templates for ribozymes that produce two output RNA fragments upon induction by a single input strand. A doubler HHR can produce two identical outputs (Homo-doubler) or it can produce two different outputs (Hetero-doubler). Homo-doublers can be used to increase the concentration of a

specific RNA strand while hetero-doublers can be used to trigger two inducible ribozymes by providing two different RNA strands. There are several doubler designs that are presented in this thesis, but the core idea is to provide two output RNA strands in response to the binding with a single ssDNA/ssRNA input strand.

Several HHR-doubler designs were conceived, the first doubler design (Figures 12 and 13) consists of two HHRs joined by Stem IIIA and Stem IB of the ribozyme A and B, respectively. Ribozyme A, with stems IA, IIA and IIIA, is an inducible ribozyme, and self-cleaves in the presence of an input DNA oligonucleotide (Figure 12 B). In contrast, ribozyme B is a constitutive ribozyme and self-cleaves without input (Figure 12 B). The resulting fragment is large and hence remains attached to the ribozyme at 37°C because of strong hydrogen bonding. After induction with the input, ribozyme A self-cleaves and produces two small fragments that leave the ribozyme (Figure 12 C). Hence, one input produces two output fragments.

Gel analysis (Figure 14) of this doubler shows that it cleaves twice in presence of input releasing two identical outputs of 22 nucleotides fragments (Figure 14). Hence, this molecule can be used to increase the concentration of the output strand in the environment. One drawback of this doubler is that it cleaves very slowly as the 22 nucleotides outputs are only detectable after 24-hours of incubation.
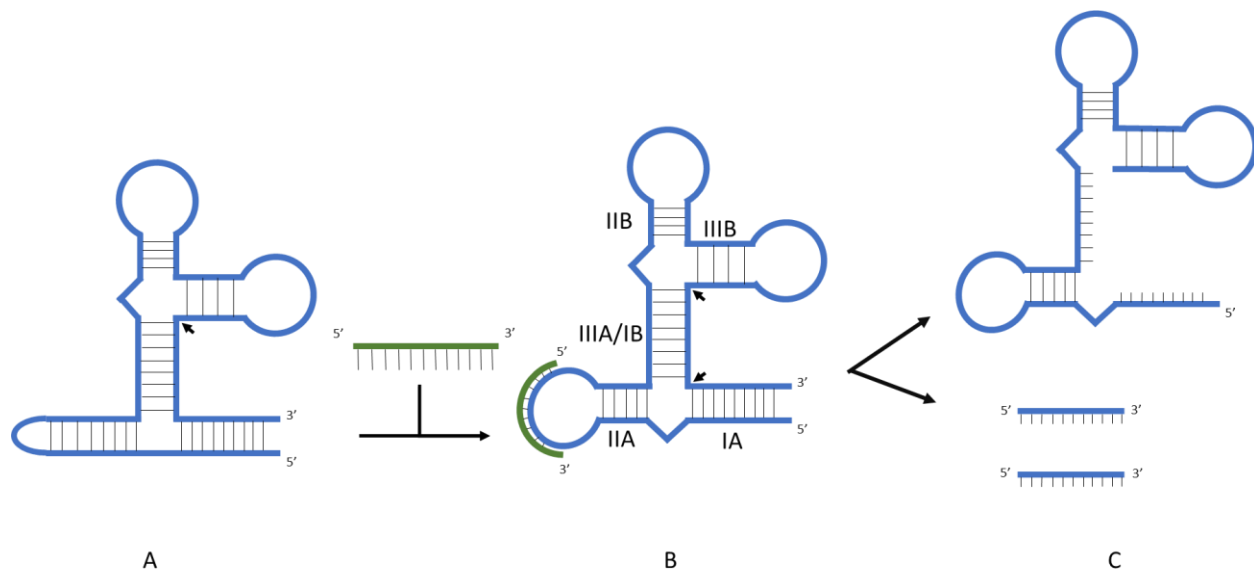
Figure 12. Two ribozyme system induced by a single input DNA strand: a 'Doubler'

(A) Inactive doubler molecule. In this molecule, ribozyme B self-cleaves as marked by a black arrow, but the output remains attached. **(B)** Introduction of an input DNA oligo (dark green strand) induces the formation of an active core in ribozyme A, resulting in another cleavage event. **(C)** After the two cleavage events, two identical or different output strands (depending on the implementation) leave the molecule, hence one input (DNA) results in two outputs (RNAs).
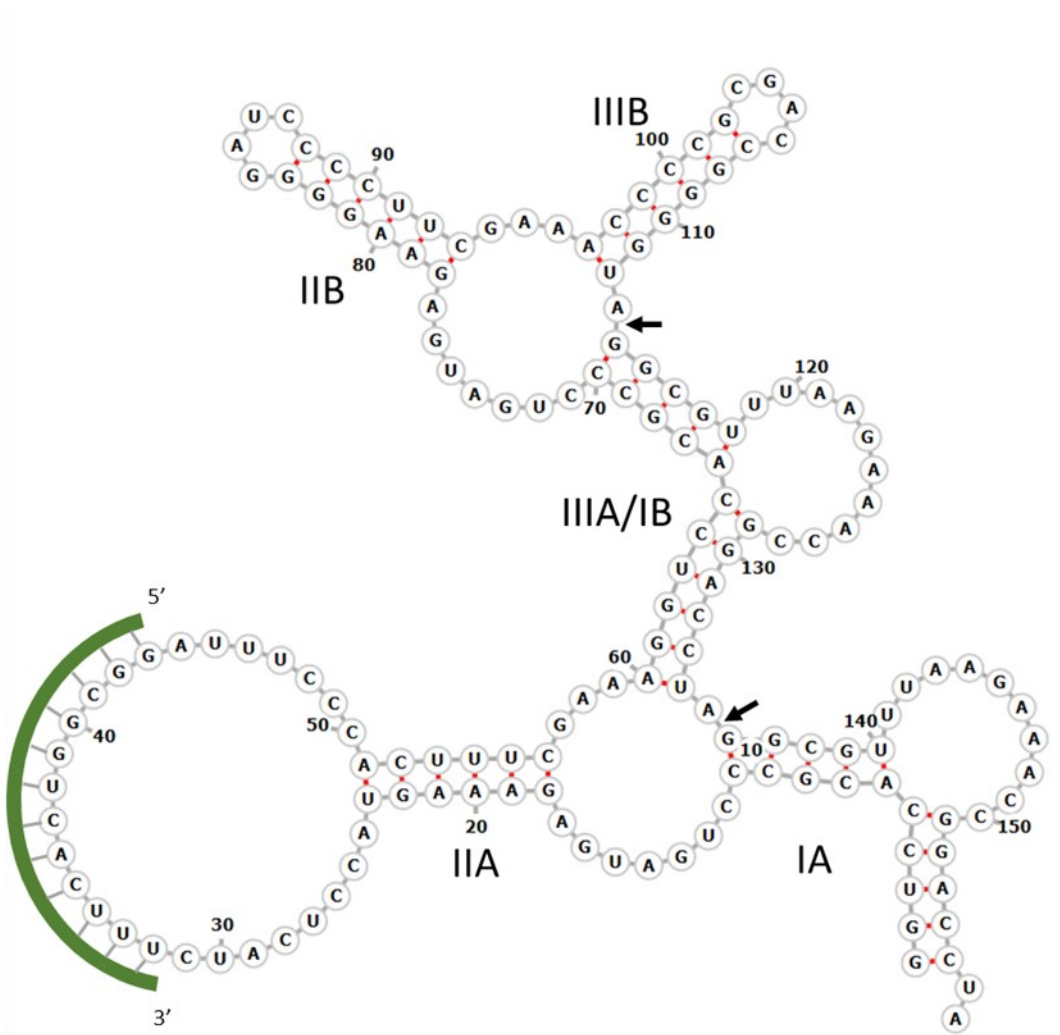
Figure 13. First doubler design (Doubler 4)

Two HHRs joined by Stem IIIA of ribozyme A and Stem IB of ribozyme B. Black arrows mark

the cleavage sites. The green input strand binds to stem IIA loop of ribozyme A
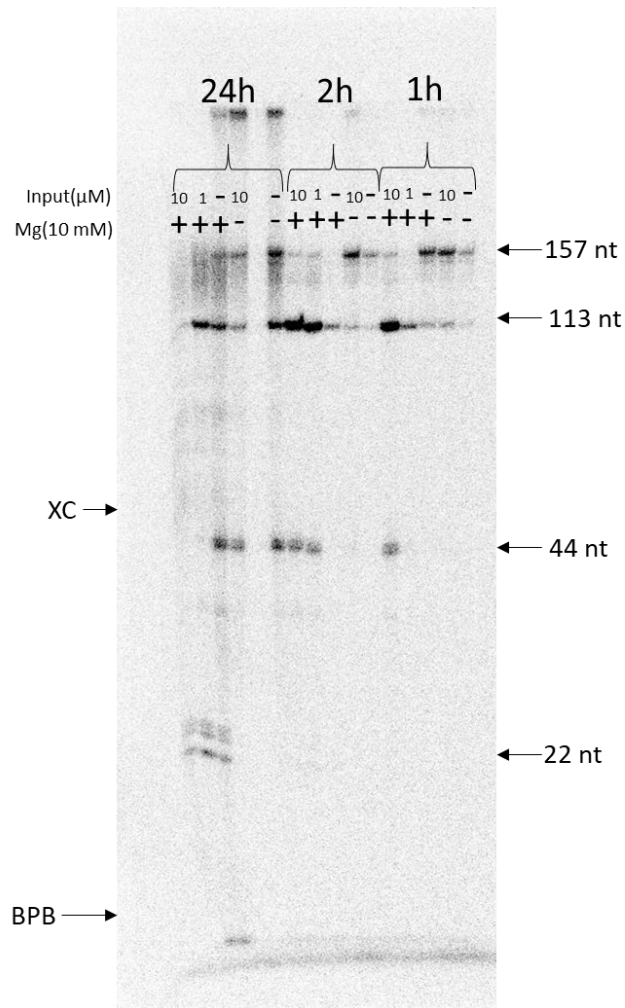
Figure 14. Doubler (Doubler 4) kinetics

Doubler 4 kinetics using [α-^{32}P] UTP labelling. Standard cleavage buffer conditions were used, and all the reactions were carried out at 37°C. Lanes are as indicated in the figure: all lanes contain ribozyme; either without (negative control) or with 10 mM MgCl$_2$; and either without input or with 1 or 10 μM (as indicated). The left side of the gel shows all expected fragment sizes.

4.5 Amplifier assay

Doubler designs can have two different purposes: to activate two different pathways upon sensing a single input molecule (hetero doublers); or to increase the concentration of an output strand (homo doublers). The latter can be used to create an RNA amplifier (Figure 15).

An RNA amplifier has two components: doubler and converter. Doubler HHRs are the key to amplification, while converter HHRs serve to activate doubler HHRs. This system is important in large molecular circuits as ribozymes are not 100% efficient in processing signals and hence, any signal will gradually grow weaker. Hence, an amplifier is needed to boost the signal, in other words, increase the concentration of specific ssRNA molecules.

To use a doubler HHR as an amplifier, doubler 1 (Appendix, Figure 22) and converter 1 (Appendix, Figure 21) were designed in a way that the output of one molecule corresponds to the input of another (Figure 15). This amplifier was tested using unlabeled RNA molecules (cold) and radiolabelled RNA molecules. In lane 4, 5 and 6, a cold converter was used to validate the amplifier and to distinguish 22 nucleotides strands from converter to doubler. Here, the reaction was started by the addition of 0.01 µM doubler input strand in lane 5 and a 0.001 µM doubler input strand in lane 6 (Figure 16). Unexpected results were obtained, as instead of amplifying the RNA output, the doubler and converter modules apparently (partially) annealed to each other. This is probably because the converter and doubler have complementary sequences, with large (open) bulges in their respective output strands (even without HHR cleavage), making output of converters and doublers available to their target Oligonucleotide Binding Sites (OBS) regardless of cleavage (Appendix Figure 21 A and 22).
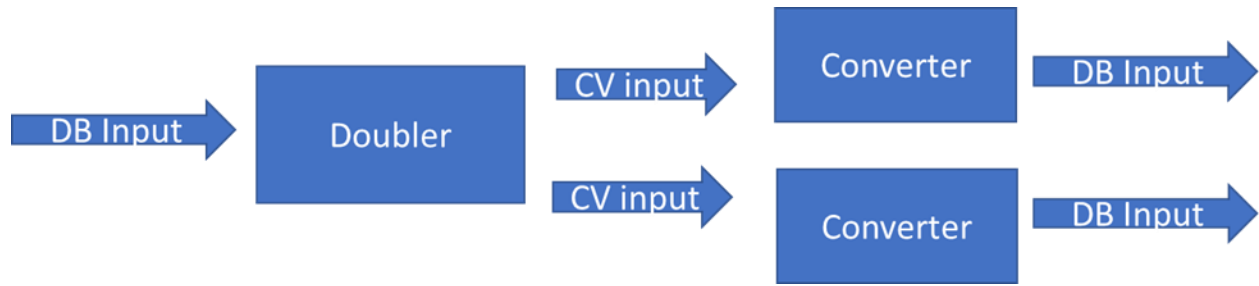
Figure 15. Schematic diagram of RNA-based amplifier.

The DB input corresponds to the doubler input, and CV input corresponds to the doubler's output, which is the same as the converter input. Upon binding with doubler input, the doubler self-cleaves twice to produce two identical ssRNAs, which act as converter inputs. Converters receiving the doubler's output proceed to self-cleave to produce doubler inputs. These inputs activate other *uncleaned* doublers, resulting in a chain reaction, leading to exponential amplification of the original DB Input.
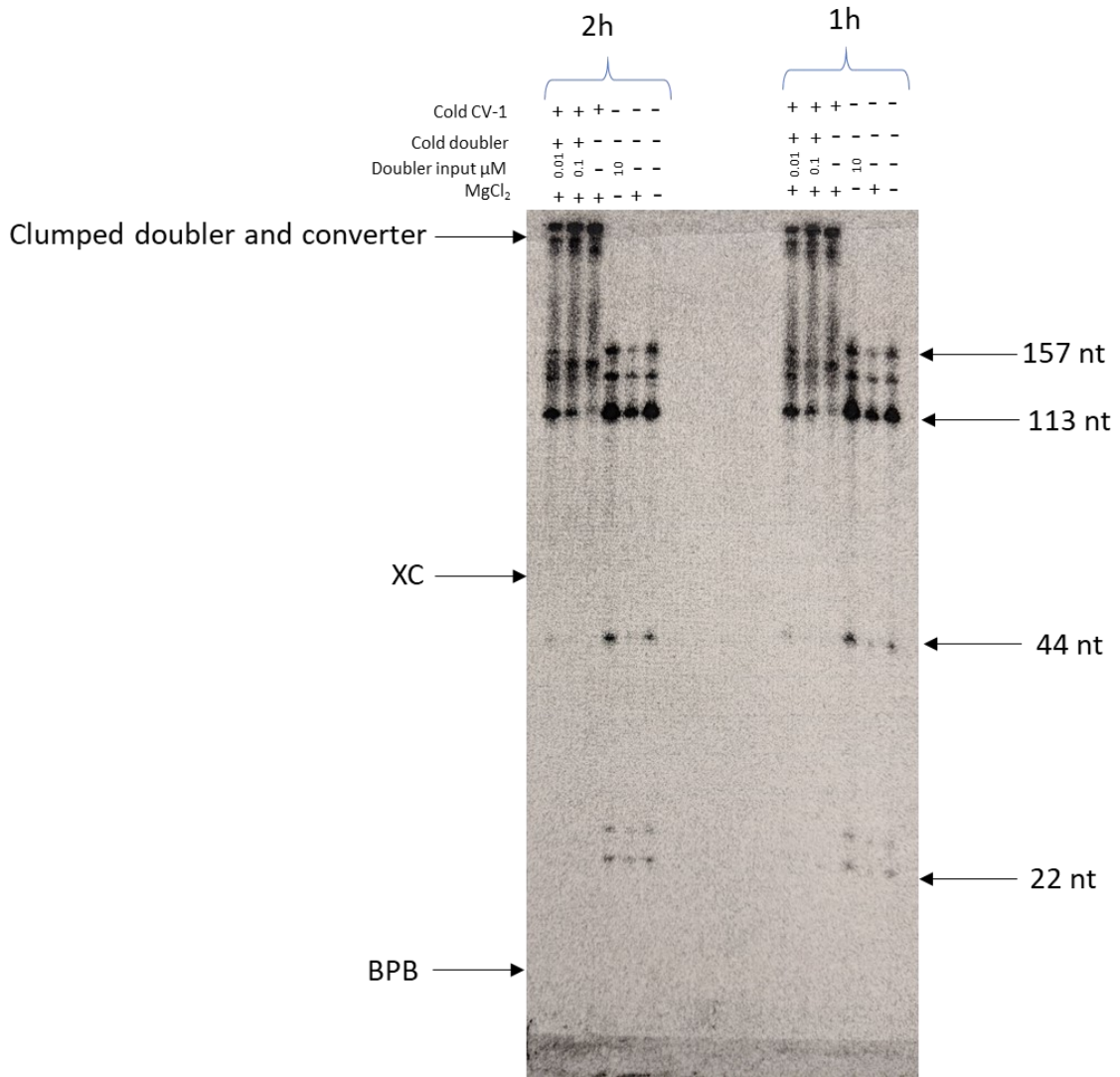
Figure 16. Amplifier testing: combination of Doubler 1 and Converter 1.
Doubler 1's output acts as an input to converter 1, while converter 1's output acts as an input to doubler 1. Standard cleavage buffer conditions were used, and all the reactions were carried out at 37°C. Lanes are as indicated in the figure: all lanes contain radiolabelled doubler 1; either with or without 10 mM MgCl$_2$; and with or without cold converter 1 or cold doubler 1 as indicated; with or without 0.01, 0.1 or 10 μM input, as indicated in figure. The left side shows all expected fragment sizes.

To avoid unexpected crosstalk between two ribozymes, new doublers and converters were designed while considering all the possible interactions. D1 and D2 doublers were designed and large bulges and loops were avoided in output strands to prevent crosstalk between doublers and converters. We did not manage to generate any sequences that would fit the requirements for the D2 doubler design but had promising candidates for D1 doubler designs. When we tried to generate D2 designs, we managed to generate ribozymes that cleaves once upon induction with input, but after first cleavage, the ribozyme was misfolded and could not cleave second time. This was due to complementary sequences in stem I and III.

4.6 D1 doubler kinetics

The second doubler design was named D1 (Figure 17 and 18). A D1 doubler is designed in a way that allows it to form a pseudoknot between Stem II loop of ribozyme 1 and Stem II loop of ribozyme 2 (Figure 17 A). Here, ribozyme 1 is type III HHR while ribozyme 2 is type I HHR. The pseudoknot formed is intended to prevent the formation of an active hammerhead core in both ribozymes, because this Stem II- Stem II interaction should prevent Stems I and II from interacting and achieving optimal conformation of the catalytic core. A linker of adenosine nucleotides (11 nucleotides) was placed between the two ribozymes to provide flexibility in forming the inactivating pseudoknot. Binding with the input on stem II of ribozyme 1 breaks off the pseudoknot, changing the conformation of the whole RNA strand and resulting in self-cleavage by both ribozymes (Figure 17 C).

D1 doubler results (Figure 19) shows that this doubler cleaves in the presence of input but also cleaves in the absence of input when Mg^{2+} is present in medium. Two HHRs, both induced by a single input DNA strand, were designed with a pseudoknot between stem II loop of ribozyme 1 and stem II loop of ribozyme 2 (Figure 19 A). The inhibitory pseudoknot is disrupted by the input

DNA strand (Figure 18 and 19 B), activating both HHR modules and leading to two self-cleavage events, generating two identical output strands (Figure 19 C). However, when generating this sequence, we accidentally allowed stem I and stem II of ribozyme 1 to form a pseudoknot. This was not intended as, generally, interaction between stem I and II allows natural ribozymes to cleave efficiently [11]. Unexpectedly, instead of cleaving itself during transcription, the ribozyme remained inactive. This may be because the normal interaction between stem I and II is not random, but rather serves to precisely adjust HHR conformation, and this unexpected pseudoknot somehow locked the ribozyme in a misfolded inactive conformation. Binding of the input strand to the stem II loop of ribozyme 1 disrupts this pseudoknot between stem I loop and stem II loop of ribozyme 1 as well as that of ribozyme 2. Even if this does not place the ribozyme in an optimal conformation, it should at least unlock it from its inactive conformation.
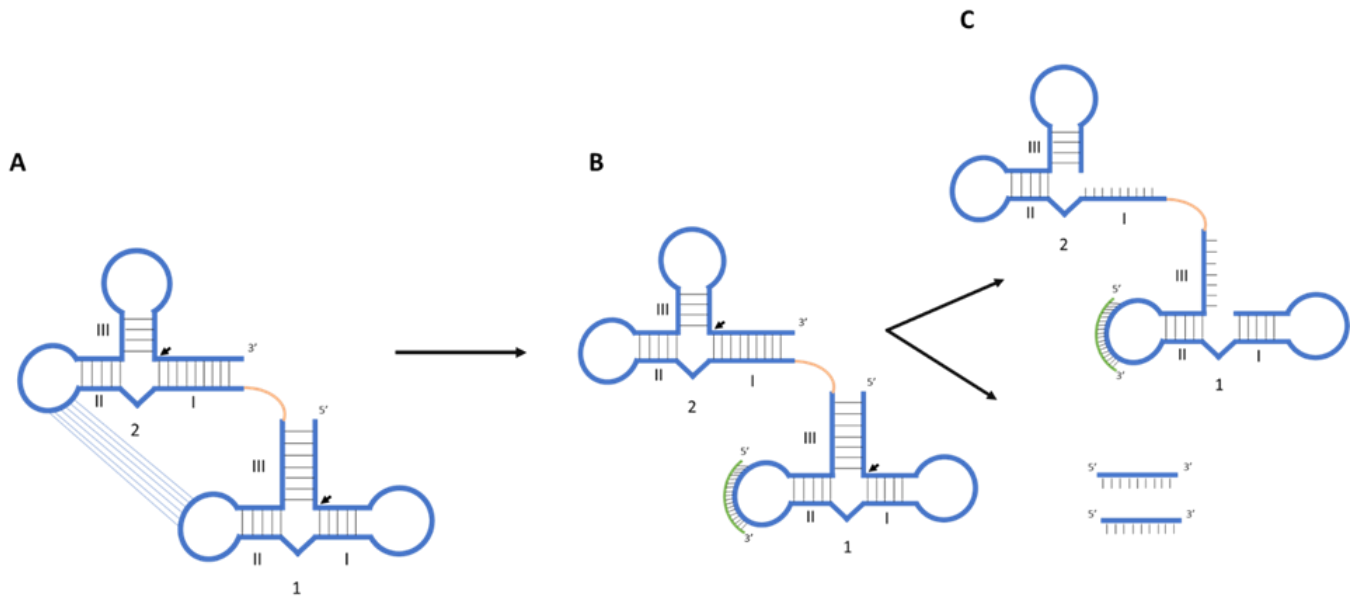
Figure 17. D1 Doubler activating scheme.

(A) D1 doubler remains inactive in the absence of input by due to a pseudoknot formed between stem II loop of ribozyme 1 and stem II loop of ribozyme 2. This pseudoknot prevents both ribozymes from self-cleaving. The two ribozymes are linked together using 11 adenosine nucleotides (orange strand). **(B)** Upon binding to the input strand (green strand) on stem II loop of ribozyme 1, both HHRs fold into active conformations. **(C)** Shown is the self-cleaved doubler bound to the input and the resulting two output strands (short blue strands).
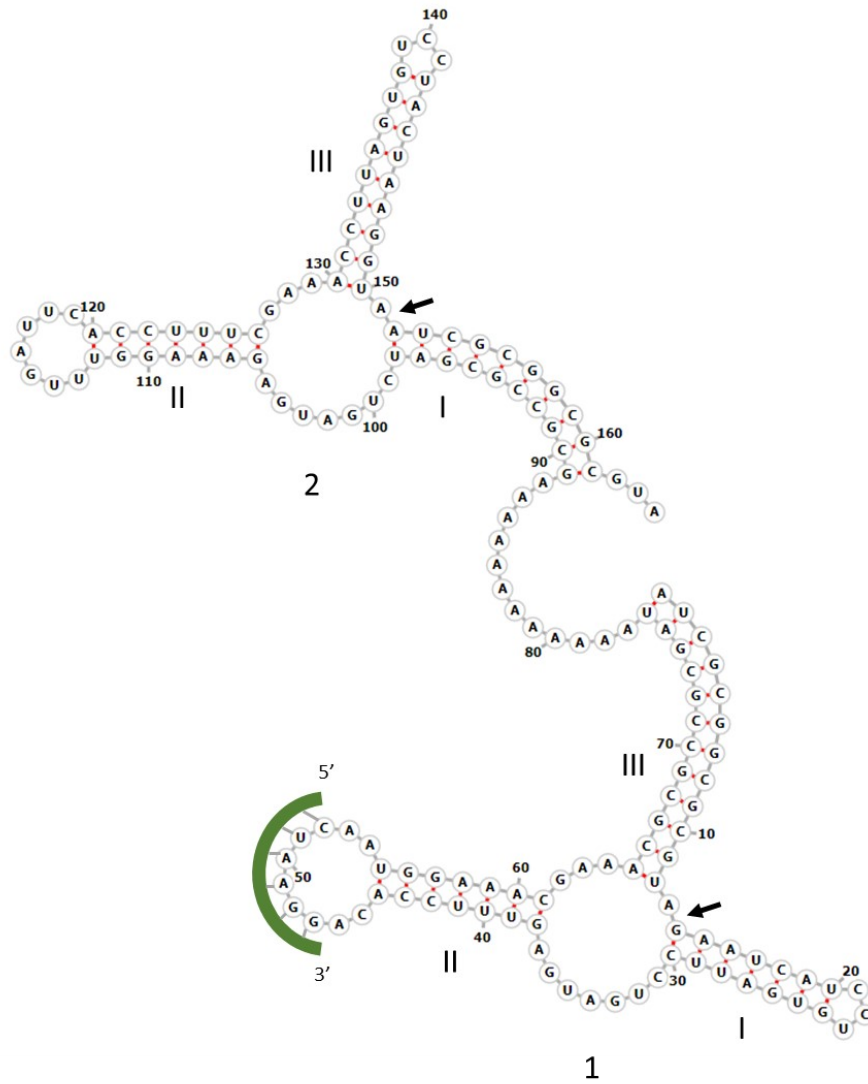
Figure 18. D1 doubler design

Two HHRs, type III and type I linked together using 11 adenine nucleotides. Both ribozymes

self-cleave at the sites marked with black arrows. Ribozyme 1 is a type III HHR while ribozyme
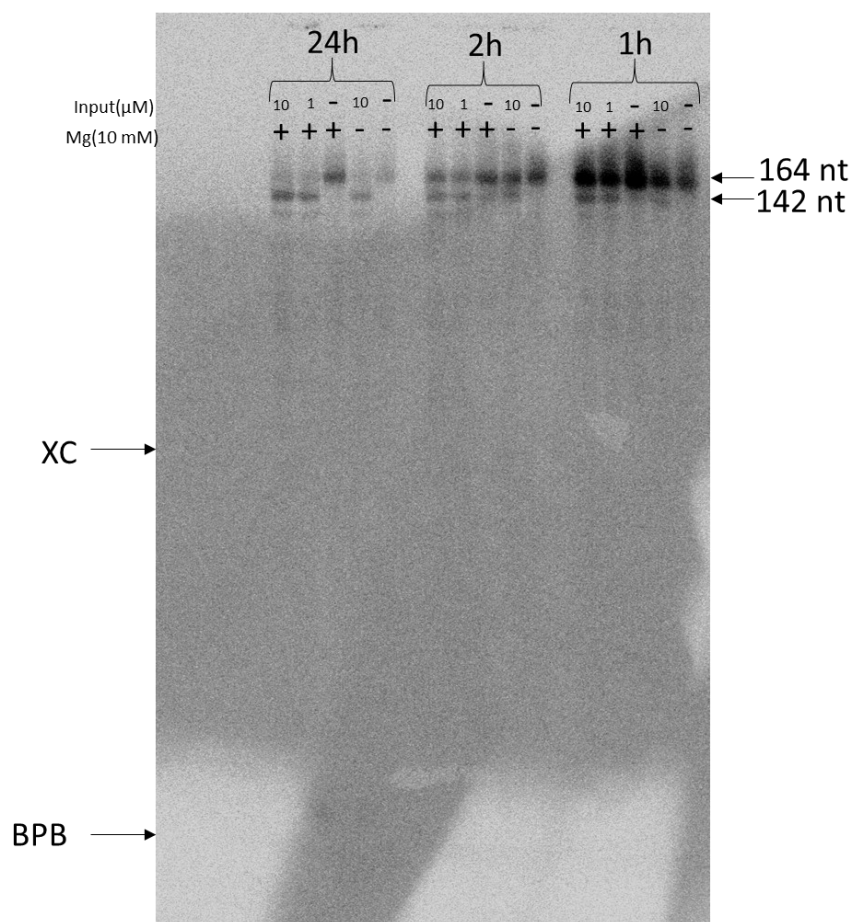
2 is a type I HHR.

Figure 19. D1 doubler kinetics.

D1 doubler was radiolabeled with [α-^{32}P] UTP during transcription. Standard cleavage buffer was used, and all reactions were carried out at 37°C. Lanes are as indicated in the figure: all lanes contain the ribozyme; either without (negative control) or with 10mM MgCl$_2$; and either without input or with 1 or 10 μM (as indicated) of input. The left side of the gel shows all expected fragment sizes.

4.7 D2 doubler design

D2 doubler design uses only one ribozyme core to catalyze two phosphoester transfer reactions, producing two output strands. The ribozyme is designed to be inducible by an input ssDNA strand. Upon binding with the input strand, the ribozyme self-cleaves, generating a short ssRNA output (Figure 20 B). After the cleavage reaction, the ribozyme refolds so the illustrated red sequence binds to stem III and the yellow strand binds to stem I (Figure 20 C). This rearrangement of the sequences leads to the formation of a new (second) hammerhead ribozyme core, leading to self-cleavage and production of a second output strand (Figure 20 D). Hence, one ribozyme molecule rearranges itself, in response to one input, to self-cleave twice, producing two output RNA strands.
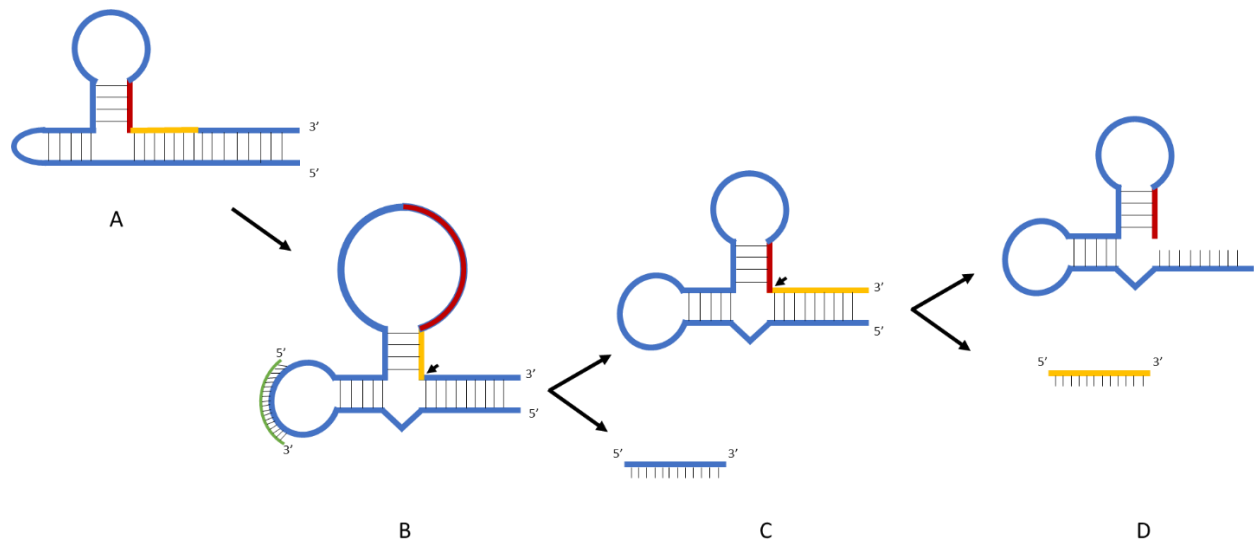
Figure 20. D2 doubler design

(A) D2 doubler in inactive state. **(B)** The ribozyme turns active upon binding to an input DNA strand (green strand) and self-cleaves to produce an output strand (blue strand). **(C)** After the first cleavage, the ribozyme refolds, and the red sequence in the loop shifts to stem II, while the yellow sequence from stem II shifts to stem I. This forms a new active hammerhead ribozyme and the resulting self-cleavage produces the second output strand. **(D)** Shown is the cleaved ribozyme along with the second output strand (in yellow), which is identical in sequence to the first output strand (in blue).

Chapter 5: Discussion, Conclusion and Future Directions

5.1 Advantages of TMSDR-based measurement of HHR activity

In the past decade, several methods have been developed and used to analyze and evaluate the structure, function, and activity of ribozymes *in vitro*. These methods include RNA radiolabeling, post-transcriptional fluorescence labelling, phosphoramidite chemistry for fluorescent labelling of chemically synthesized RNA and engineered fluorescent aptamers (e.g., Spinach and Mango) [5, 21, 22, 44, 45]. These methodologies make use of transcriptional incorporation of $[\alpha\text{-}^{32}P]$ UTP, 5′ incorporation of ^{32}P from $[\gamma\text{-}^{32}P]$ ATP or fluorophore, chemical synthesis of RNA and fluorescence activity of aptamers [5, 20, 21, 45]. However, besides radiolabeling, which has some disadvantages, these methods are associated with *direct RNA modification*, which in turn can impact structure, function and thermodynamic stability of the measured ribozyme [21, 23].

In this study, we present a novel approach for HHR cleavage kinetics that utilizes the toehold mediated strand displacement reaction (TMSDR). The proposed method separates the detection system from the ribozyme, *eliminating the need for ribozyme labeling and modification*. This fosters unhindered determination of ribozyme kinetics.

We conceived an oligonucleotide activated HHR, which functions as a YES logic gate (or *converter*). When the HHR binds to the input oligonucleotide, the HHR cleaves itself generating an ssRNA fragment that can detach from the HHR. A detached output ssRNA interacts with the toehold present on a dsDNA probe at the 3′ end of the F-strand. This binding initiates a strand displacement reaction favoring the expulsion of the quencher (Q-strand) in a 5′ to 3′ direction. This process dissociates the quencher from the fluorophore, resulting in detectable fluorescence.

The vast majority of previous studies determine HHR cleavage using radiolabeling and product separation [6, 11, 17, 45]. Product separation on denaturing gels is associated with forced detachment of an output strand from the HHR. Consequently, this approach *fails to distinguish* between released output and cleaved but bound output. However, in TMSDR, the occurrence of fluorescence is *a direct indication of released output*. An increase in cleaved product over time was noted in both (gel and TMSDR) methods for the converter 2. However, a decrease in cleavage activity from TMSDR was observed in case of Ribozyme+2bp and Ribozyme+14bp, compared to their gel counterparts. This decrease in activity is correlated with an increase in the strength of binding between the cleaved output strand and its complement (on stem I) of the ribozyme. This decreased activity is indicative that TMSDR-based fluorescence is a measure of the concentration of the *detached* output strand, rather than the full extent of ribozyme self-cleavage. Thus, TMSDR allows for *real-time cleavage monitoring and realistic evaluation of the amount of product* (RNA output) leaving the ribozyme, rather than mere cleavage.

Therefore, our approach allows for measurement of released output which, incidentally, is more important than cleavage itself for many synthetic biology applications. Furthermore, when combined with more traditional radiolabeling methods, it can help provide a *complete picture* of cleavage activity and rate of dissociation of the cleaved-products, information that can be crucial to determining and characterizing the limiting step for the development of ribozyme-based RNA circuits. TMSDR lends itself, much more readily, to automation compared to radiolabeling; a trait particularly useful for eventual design of more complex RNA logic gates and circuits and experiment-automating microfluidics devices.

5.2 Doubler HHRs and amplifiers

As described earlier, the concentration of the detached output strand is probably, in most cases, lower than what is indicated by gel. This creates a problem for other RNA-based devices that use that output strand as activating inputs for their own operations. To solve this problem, we designed different *doublers* to amplify one RNA/DNA input into more than 1 (ideally, two) RNA outputs. As these doubler HHRs self-cleave twice and even if their efficiency is not optimal, doublers can still manage to increase the concentration of output. This doubler HHR can also be used to design an *RNA amplifier* as described in Figure 15. The first amplifier design failed under testing because of the crosstalk between the doubler and its respective converter. Another problem with the first doubler design (Figure 12 A) was the purification on native gel in a cold room. As one of the ribozymes is always active, for the 44 nucleotides sequence (consisting of two outputs not yet cleaved) to stay hybridized to the ribozyme through hydrogen bonding, denaturing gel cannot be used or else it would separate the HHR from its substrate, and hence make the doubler unusable. Purification on native gel is difficult and using radioactivity in a cold room with a shield is cumbersome. Hence, we designed two more and different doublers: D1 and D2. D1 doubler sequences were generated and were tested. One of the sequences showed potential but more optimization is needed to generate a perfect D1 doubler. Interestingly, unintentional interaction between stem I and II to inhibit ribozyme cleavage was never used to design inducible HHRs and it opens new ways to design inducible HHRs. D2 design was more complex and hence we failed to generate any sequence of that design. As described earlier, D2 design has complementary sequences in stem I and stem III to allow for rearrangement and refolding. Hence, after first cleavage, it misfolds and does not cleave second time.

5.3 Future work

There are two ways to expand this project. One direction is to develop a method to design D2 doubler sequences. The D2 doubler has a lot of potential as in theory, you can make N number of sequences in stem III loop (Figure 20 B), resulting in multiple self-cleavage events (tripler or quadrupler!). As this design is compact and uses one core to cleave multiple times, it is easy to manipulate and transcribe *in vitro*.

Another possibility is the development of D1 designs, which utilize a tertiary interaction between stem I and stem II of ribozyme 1. This opens up more ways to design inducible HHRs that are more efficient upon induction by input and would significantly reduce reaction time. These new developed ribozymes can be used to develop RNA amplifiers or hetero-doublers.

It is also possible to develop the work presented herein, further, by fine-tuning and extending the TMSDR approach, so it works more efficiently and applies to other ribozymes, besides the hammerhead.

Finally, TMSDR reactions can be automated, using novel biological techniques utilized by custom-made microfluidics devices, to screen very large numbers of ribozyme sequences for logical functioning and cleavage efficiency; something that is not possible with conventional bench-top approaches.

REFERENCES

1.   Brunstein, J., *DNA and RNA structure: nucleic acids as genetic material.* MLO: Medical Laboratory Observer, 2013. **45**(1): p. 26-28.

2.   lumen Microbiology. *Structure and Function of RNA*. [cited 2020 25/03]; Available from: https://courses.lumenlearning.com/microbiology/chapter/structure-and-function-of-rna/.

3.   Varani, G. and W.H. McClain, *The G·U wobble base pair.* EMBO reports, 2000. **1**(1): p. 18-23.

4.   Cox, M.M. and D.L. DNelson, *Principles of Biochemistry* 5 ed. 2011, New York, USA: Sara Tenney.

5.   Auslander, S., et al., *Engineering a ribozyme cleavage-induced split fluorescent aptamer complementation assay*. 2016.

6.   Hammann, C., et al., *The ubiquitous hammerhead ribozyme.* RNA, 2012. **18**(5): p. 871-85.

7.   Puerta-Fernández, E., et al., *Ribozymes: recent advances in the development of RNA tools.* FEMS Microbiology Reviews, 2003. **27**(1): p. 75-97.

8.   Eckstein, F. and D.M.J. Lilley, *Ribozymes and RNA Catalysis*. RSC Biomolecular Sciences. 2008, Cambridge: Royal Society of Chemistry.

9.   Wrzesinski, J., et al., *Catalytic cleavage of cis- and trans-acting antigenomic delta ribozymes in the presence of various divalent metal ions.* Nucleic Acids Research, 2001. **29**(21): p. 4482-4492.

10. Scott, W.G., L.H. Horan, and M. Martick, *The hammerhead ribozyme: structure, catalysis, and gene regulation.* Progress in molecular biology and translational science, 2013. **120**: p. 1-23.

11. Perreault, J., et al., *Identification of hammerhead ribozymes in all domains of life reveals novel structural variations.* PLoS computational biology, 2011. **7**(5): p. e1002031-e1002031.

12. Anderson, M., et al., *Active-Site Monovalent Cations Revealed in a 1.55-Å-Resolution Hammerhead Ribozyme Structure.* Journal of Molecular Biology, 2013. **425**(20): p. 3790-3798.

13. Lee, T.-S., et al., *Role of Mg2+ in Hammerhead Ribozyme Catalysis from Molecular Simulation.* Journal of the American Chemical Society, 2008. **130**(10): p. 3053-3064.

14. Khvorova, A., et al., *Sequence elements outside the hammerhead ribozyme catalytic core enable intracellular activity.* Nature Structural Biology, 2003. **10**(9): p. 708-712.

15. De la Peña, M., S. Gago, and R. Flores, *Peripheral regions of natural hammerhead ribozymes greatly increase their self-cleavage activity.* The EMBO Journal, 2003. **22**(20): p. 5561-5570.

16. O'Rourke, S.M., W. Estell, and W.G. Scott, *Minimal Hammerhead Ribozymes with Uncompromised Catalytic Activity*. 2015. p. 2340-2347.

17. Penchovsky, R. and R.R. Breaker, *Computational design and experimental validation of oligonucleotide-sensing allosteric ribozymes.* Nature Biotechnology, 2005. **23**(11): p. 1424-1433.

18. Kharma, N., et al., *Automated design of hammerhead ribozymes and validation by targeting the PABPN1 gene transcript.* Nucleic Acids Research, 2015. **44**(4): p. e39-e39.

19. Margolin, A.A. and M.N. Stojanovic, *Boolean calculations made easy (for ribozymes).* Nature Biotechnology, 2005. **23**(11): p. 1374-6.

20. Singh, K.K., R. Parwaresch, and G. Krupp, *Rapid kinetic characterization of hammerhead ribozymes by real-time monitoring of fluorescence resonance energy transfer (FRET).* 1999. p. 1348-1356.

21. Li, N., C. Yu, and F. Huang, *Novel cyanine-AMP conjugates for efficient 5' RNA fluorescent labeling by one-step transcription and replacement of [γ-32P]ATP in RNA structural investigation.* Nucleic Acids Research, 2005. **33**(4): p. e37-e37.

22. Debiais, M., et al., *Splitting aptamers and nucleic acid enzymes for the development of advanced biosensors.* Nucleic Acids Research, 2020.

23. Moreira, B.G., et al., *Effects of fluorescent dyes, quenchers, and dangling ends on DNA duplex stability.* Biochemical and Biophysical Research Communications, 2005. **327**(2): p. 473-484.

24. Mikulecky, P.J. and A.L. Feig, *Heat capacity changes in RNA folding: application of perturbation theory to hammerhead ribozyme cold denaturation.* Nucleic acids research, 2004. **32**(13): p. 3967-3976.

25. Penchovsky, R. and R. Breaker, *Penchovsky, R. & Breaker, R. R. Computational design and experimental testing of oligonucleotide-sensing allosteric ribozyme. Nature Biotechnol. 23, 1424-1433.* Nature biotechnology, 2005. **23**: p. 1424-33.

26. Mujumdar, R.B., et al., *Cyanine dye labeling reagents: Sulfoindocyanine succinimidyl esters.* Bioconjugate Chemistry, 1993. **4**(2): p. 105-111.

27. Simmel, F.C., B. Yurke, and H.R. Singh, *Principles and Applications of Nucleic Acid Strand Displacement Reactions.* 2019. p. 6326-6369.

28. Aakriti Alisha, A. and S. Chamaree de, *Beyond the smiley face: applications of structural DNA nanotechnology.* Nano Reviews & Experiments, 2018(1).

29. Venkataraman, S., et al., *An autonomous polymerization motor powered by DNA hybridization.* Nature Nanotechnology, 2007. **2**(8): p. 490-494.

30. Qian, L., E. Winfree, and J. Bruck, *Neural network computation with DNA strand displacement cascades.* Nature, 2011. **475**(7356): p. 368-372.

31. Wang, B., et al., *Effective design principles for leakless strand displacement systems.* Proceedings of the National Academy of Sciences, 2018. **115**(52): p. E12182.

32. Zhang, D.Y. and E. Winfree, *Control of DNA Strand Displacement Kinetics Using Toehold Exchange.* Journal of the American Chemical Society, 2009. **131**(47): p. 17303-17314.

33. David Yu, Z. and G. Seelig, *Dynamic DNA nanotechnology using strand-displacement reactions.* Nature Chemistry, 2011. **3**(2): p. 103-113.

34. Šulc, P., et al., *Modelling toehold-mediated RNA strand displacement*. 2014.

35. Duose, D.Y., et al., *Configuring robust DNA strand displacement reactions for in situ molecular analyses.* Nucleic acids research, 2012. **40**(7): p. 3289-3298.

36. Ravan, H., et al., *Dual catalytic DNA circuit-induced gold nanoparticle aggregation: An enzyme-free and colorimetric strategy for amplified detection of nucleic acids.* International Journal of Biological Macromolecules, 2020.

37. Khodakov, D.A., et al., *Protected DNA strand displacement for enhanced single nucleotide discrimination in double-stranded DNA.* Scientific Reports, 2015. **5**(1): p. 8721.

38. *Computational design of inducible hammerhead ribozyme sequences* J. Kapadia, Editor. 2018, August, 18, Nickolas kamel p. 3.

39. Lorenz, R., et al., *ViennaRNA Package 2.0.* Algorithms for Molecular Biology, 2011. **6**(1): p. 26.

40. Deb, K., et al., *A fast and elitist multiobjective genetic algorithm: NSGA-II.* IEEE Transactions on Evolutionary Computation, 2002. **6**(2): p. 182-197.

41. Tian, S. and R. Das, *Primerize-2D: automated primer design for RNA multidimensional chemical mapping.* Bioinformatics, 2017. **33**(9): p. 1405-1406.

42. Kerpedjiev, P., S. Hammer, and I.L. Hofacker, *Forna (force-directed RNA): Simple and effective online RNA secondary structure diagrams.* Bioinformatics, 2015. **31**(20): p. 3377-3379.

43. Furth, J. and J.L. Tullis, *Carcinogenesis by radioactive substances.* Cancer research, 1956. **16**(1): p. 5-21.

44. Mitra, J. and T. Ha, *Nanomechanics and co-transcriptional folding of Spinach and Mango.* Nature Communications, 2019. **10**(1): p. N.PAG.

45. Porecha, R. and D. Herschlag, *Chapter Fourteen - RNA Radiolabeling*, in *Methods in Enzymology*, J. Lorsch, Editor. 2013, Academic Press. p. 255-279.

Appendix

Converter sequences with their actual secondary structure
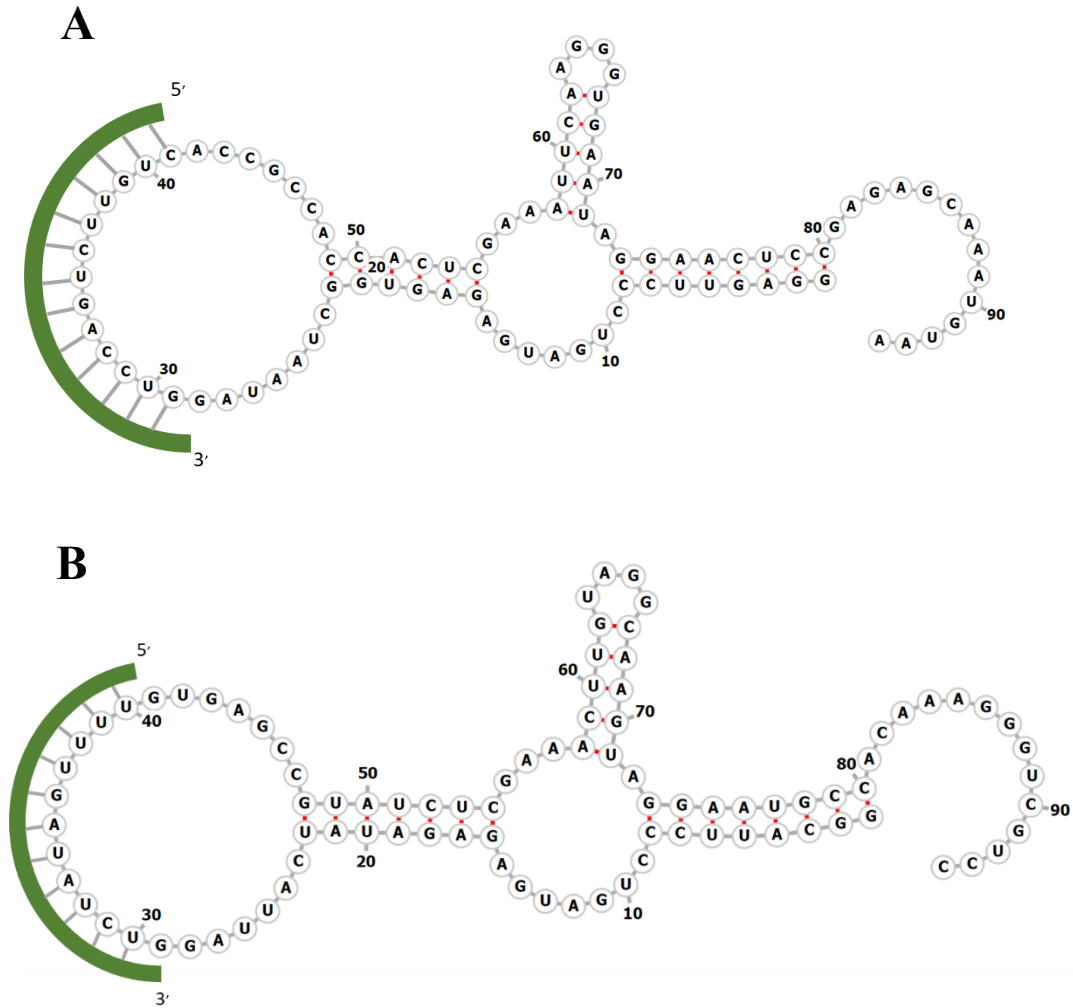
A

B

Figure 21. Converter 1 and 3 active secondary structures

Both secondary structure were generated from *Forna RNA* [42].

(A) Converter 1 active structure bound with input DNA strand (dark green) **(B)** Converter 3 active secondary structure bound with input DNA strand (dark green).

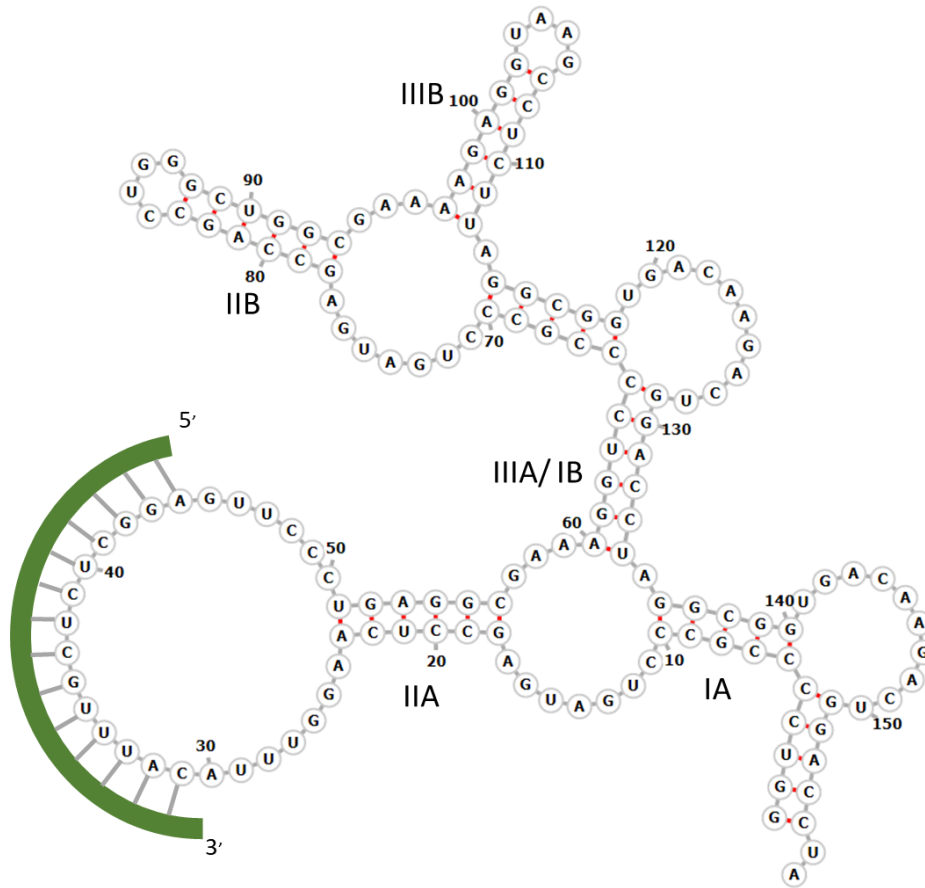**Doubler sequence with predicted secondary structure**

Figure 22. Doubler 1 secondary structure

Dark green strand represents input DNA oligonucleotide that binds with the stem II loop of

Ribozyme A

Pseudoknot converter design

Another converter (YES logic gate) was designed by forcing tertiary interaction (pseudoknots) between stem II loop and stem III loop of HHR. (Figure 23). Unfortunately, none of the designs worked.
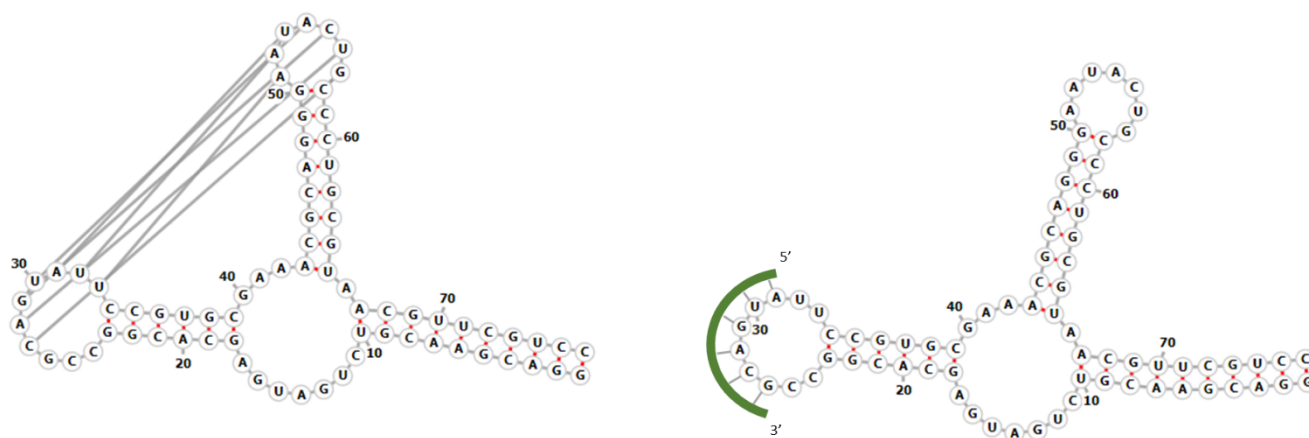

Figure 23. Pseudoknot converter design

Left side shows the pseudoknot between stem II loop and stem III loop. Right side sequence shows the induction of riozyme when bind with input (dark green strand) on stem II loop.

Summary table of all the tested sequences

Name	Gate type	During transcription	Rz	Rz+ Mg^{2+}	Rz+Input	Rz+Mg^{2+} input
Converter-1	YES	No cleavage	No cleavage	No cleavage initially but cleaves after 24 hours	No cleavage but cleaves slightly after 24 hours	Significant cleavage
Converter-2	YES	Slightly cleaving	No cleavage	Cleaves little bit after 2 hours but significant cleavage after 24 hours	No cleavage but cleaves slightly after 24 hours	Significant cleavage
Converter-3	YES	No cleavage	No cleavage	No cleavage but significant cleavage after 24 hours	No cleavage but cleaves slightly after 24 hours	Significant cleavage
Converter-4	YES	No cleavage	No cleavage	No cleavage but Significant cleavage after 24 hours	No cleavage but cleaves slightly after 24 hours	Significant cleavage
Doubler-1	doubler	No cleavage	little bit	Significant cleavage even after 2 hours	More cleavage than with Mg^{2+}	Significant cleavage
Doubler-2	doubler	Significant cleaving	Not tested as already active	Not tested as already active	Not tested as already active	Not tested as already active
Doubler-3	doubler	Significant cleavage	Not tested as already active	Not tested as already active	Not tested as already active	Not tested as already active
Doubler-4	doubler	No cleavage	No but cleaves after 24 hours	Cleaves little bit after 2 hours but cleaves after 24 hours	Cleaves little bit after 24 hours	significant cleavage after 24 hours
D1 doubler	Doubler	Slight cleavage	No cleavage	Cleaves little bit	Cleaves little bit	Significant cleavage after 2 hours

Table 7. Summary table for all tested sequences

During transcription= Cleavage observed during 10 % PAGE purification. Rz= Ribozyme in

cleavage buffer (as described in materials and methods) without Mg^{2+} and input DNA
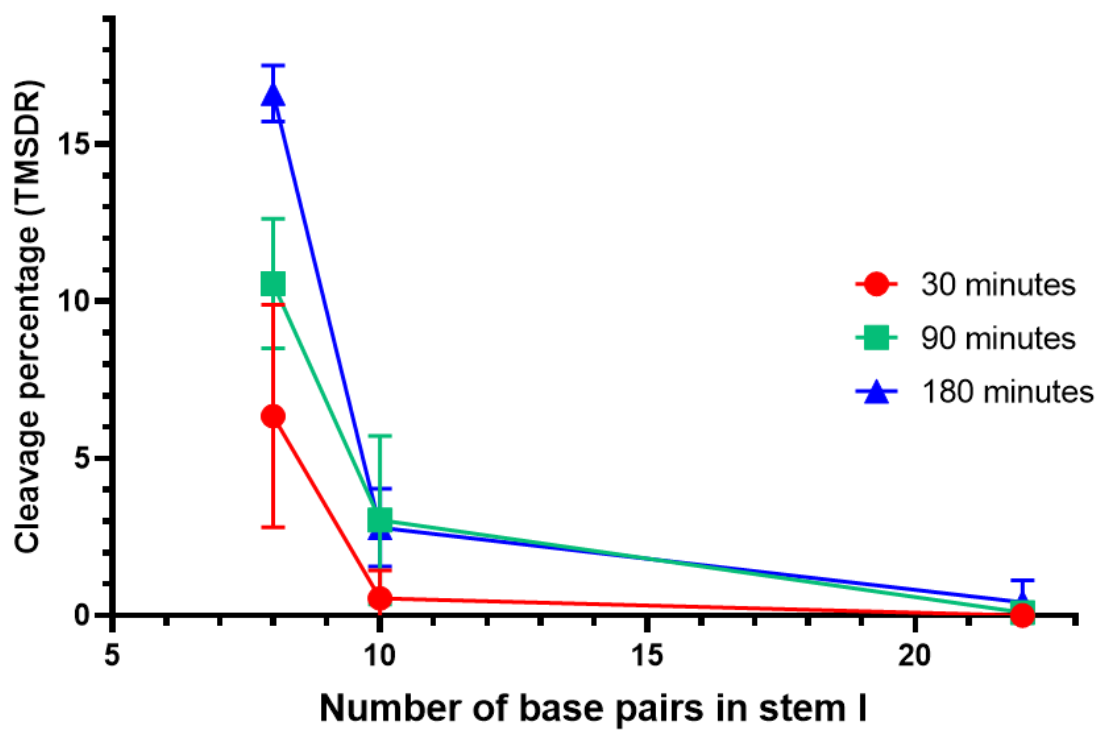
oligonucleotide.

Figure 24. Comparison of cleavage observed from TMSDR as the number of base pairs increase
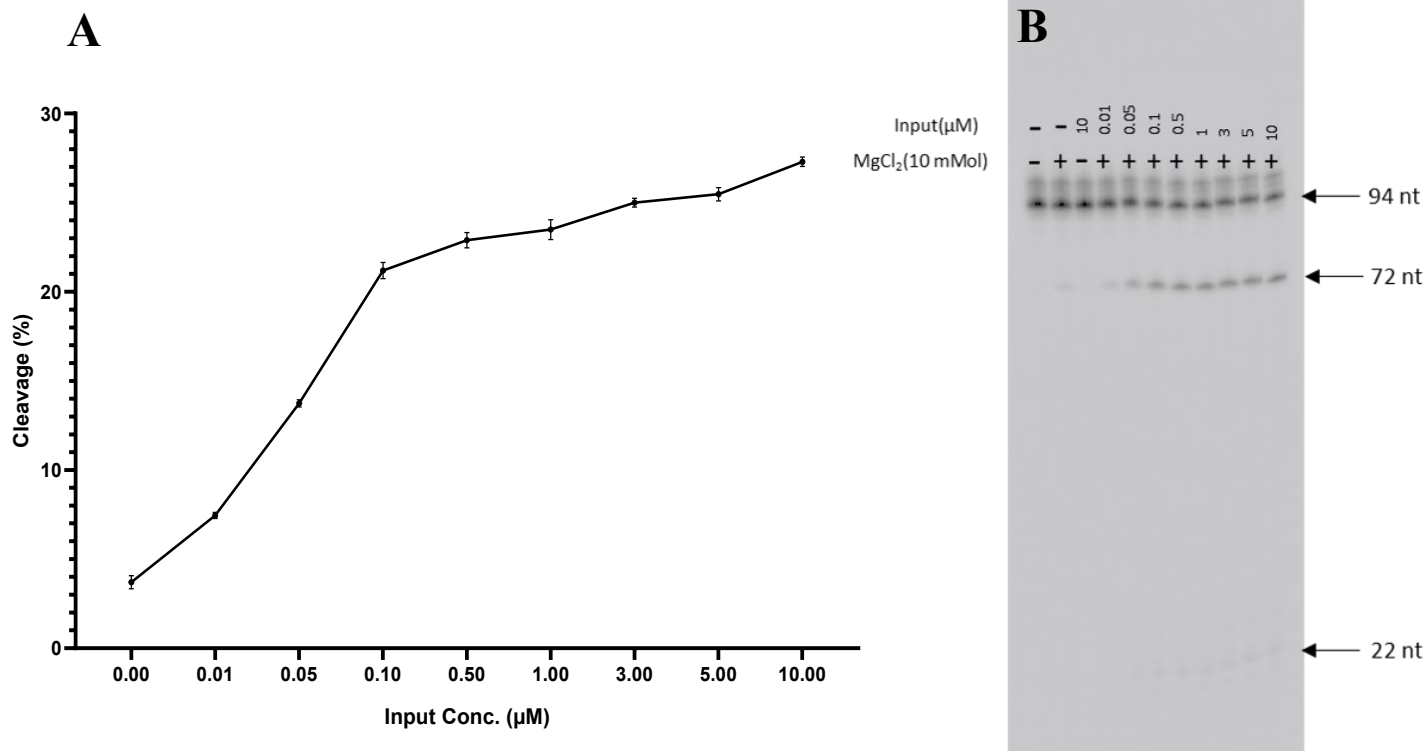
in stem I.

Figure 25. Cleavage observed as a function of input DNA oligonucleotide concentration for converter 2.

All samples were incubated for 2 hours in standard cleavage conditions. **(A)** Graphical representation of the curve showing increase in cleavage as function of input DNA oligonucleotide concentration. **(B)** Gel image showing cleavage of converter-2 in different conditions.
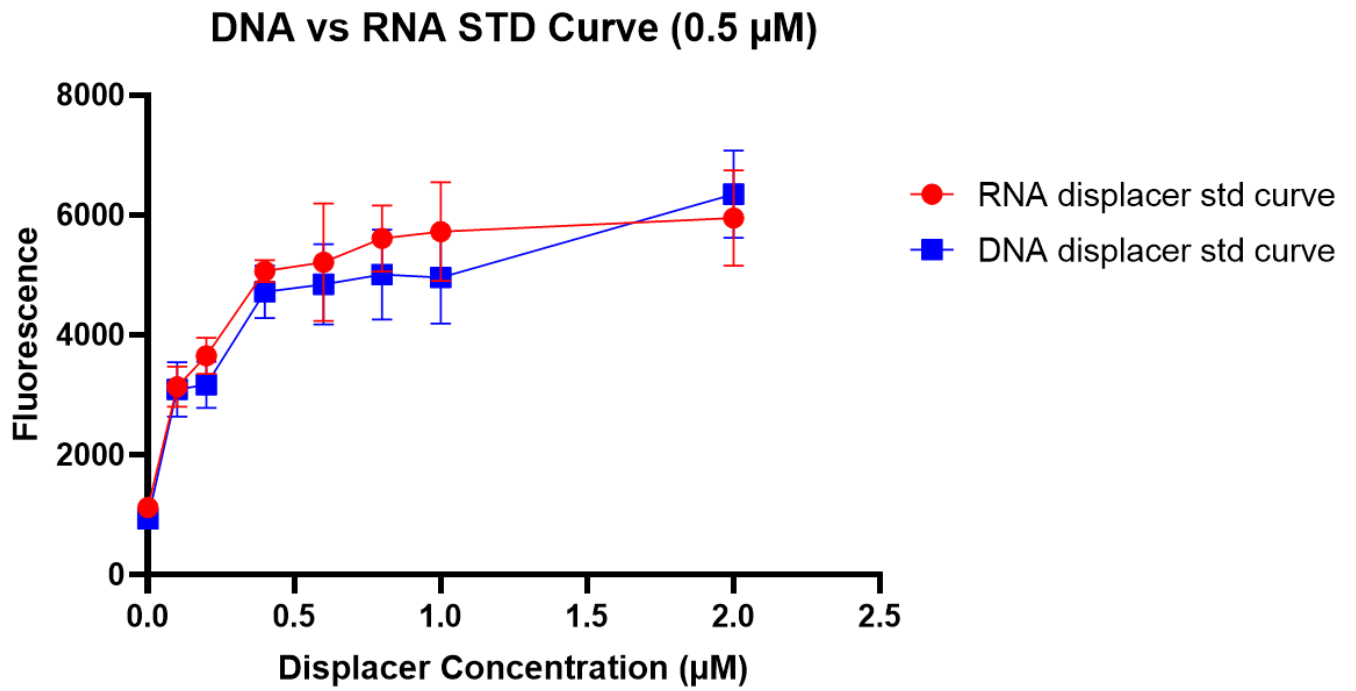
Figure 26. Standard curve comparison using DNA and RNA as displacer in same conditions and
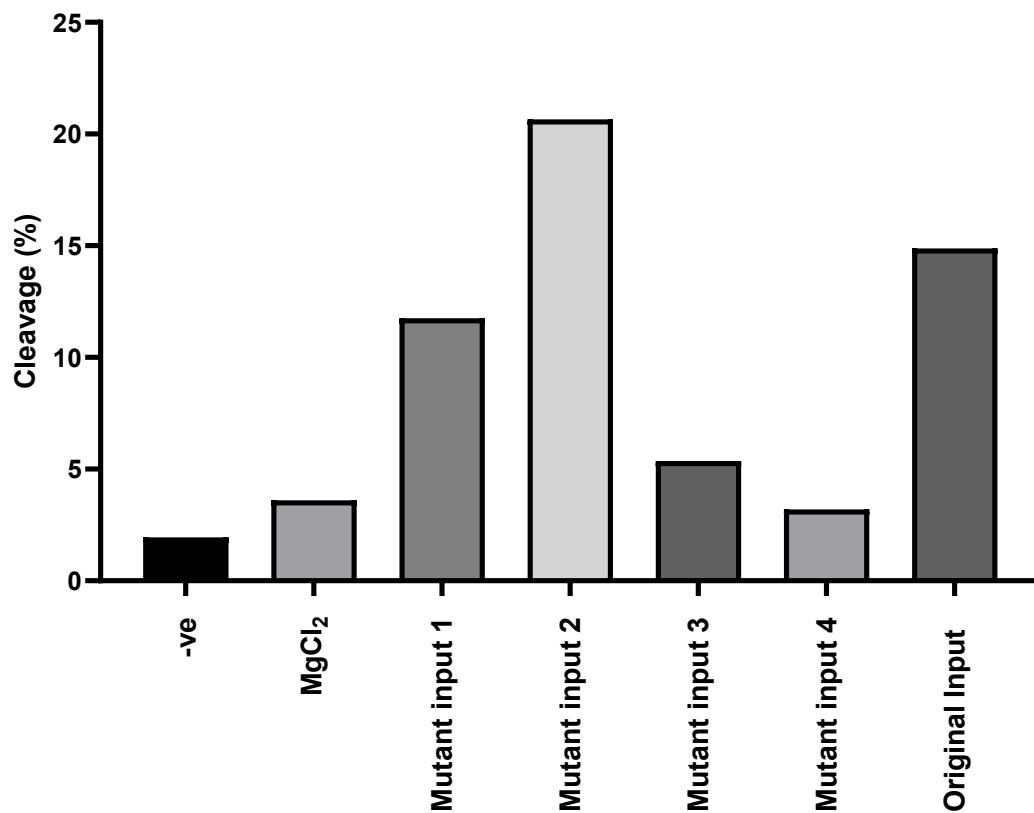
from same reaction mixture.

Figure 27. Converter 2 assay in the presence of different mutant inputs.

Standard cleavage conditions were used, and all the samples were incubated for 2 hours at 37°C.

10 µM of each input DNA oligonucleotide were used in this assay.